

1 **Response to reviewers**

2 *We are **grateful and thank** Reviewer#1 and Reviewer#2 for thorough assessment of our manuscript and*  
3 *for providing us constructive comments and suggestions.*

4 *In the revised version, **all the comments and suggestions have been taken into account** and changes*  
5 *have been made to improve the presentation.*

6 *We now add point-by-point reply (in italics, in red color fonts) to the comments and suggestions of the*  
7 *reviewers and make clear where and what changes have been made in the revised version of the*  
8 *manuscript.*

9 *Please note that the (1) comments from referees, (2) author's response, and (3) author's changes in*  
10 *manuscript are all described below. The marked-up manuscript version has been added after the response*  
11 *section.*

12

13 **Reviewer #1**

14 **Comment.** This manuscript reports on the differences between gullies formed on different substrates on  
15 Mars. Martian gullies are widespread, relatively young, features in the mid-latitudes, with similarities  
16 with some types of gully on Earth. Given the possibility of debris-flow processes being present, these  
17 features are important in attempts to understand fluidization processes on Mars. The manuscript is a  
18 timely addition to body of work on martian gullies.

19 Overall the manuscript is excellent, and it is a pleasure to say that I think that it should be accepted without  
20 any changes. The justification for this recommendation is that the study is well-designed, has been carried  
21 out to an excellent standard, interpretations are sound without speculation, and the conclusions make a  
22 solid contribution to our understanding of martian gullies.

23 **Response:** *We sincerely thank the reviewer for this assessment and providing a summary of our paper.*  
24 *We acknowledge the reviewer for providing a positive feedback on our manuscript.*

25

26 **Reviewer #2**

27 **Overall comments (see attached supplement for figures)**

28 **Comment 1:** Overall the manuscript is well-written and with some minor improvements will be a nice  
29 contribution to the field. The manuscript could use more discussion about the significance of the results.

30 As written it is not really clear why it matters that there is a morphologic distinction between gullies  
31 carved into bedrock and mantling.

32 Most of the discussion is about comparing the morphometry of martian gullies with gullies on Earth, and  
33 doesn't really involve the bedrock/LDM distinction at all.

34 ***Response 1.** Morphological distinction between gullies formed in the bedrock and LDM signifies that  
35 Martian gullies may have multiple formative mechanisms. Bedrock gullies would have formed by  
36 mechanisms unrelated to LDM. For instance, alcoves of the bedrock gullies have a crenulated shape,  
37 suggesting possibility of headwards erosion into the crater rim. The alcoves are composed of multiple  
38 sub-alcoves. Whereas, gullies in association with LDM have elongated alcoves that are V-shaped in  
39 cross-section, indicating presence of ice-rich unlithified sediments constituting the LDM. The elongated  
40 V-shaped cross-section could be related to the fine-grained, loosely packed, unconsolidated materials  
41 within LDM. Accordingly, we have found that the estimated length of alcoves formed in LDM/glacial  
42 deposits is found to be relative higher than that of alcoves formed in bedrock. This discussion is already  
43 there in the section 5.1, lines 274-290 of the revised version.*

44 *The comparison between combinations of Melton ratio with alcove length and fan gradient of terrestrial  
45 and Martian gullies suggest that the Martian gully systems studied in this work were likely dominated by  
46 terrestrial debris-flow like processes during their formation.*

47 *In the revised manuscript, based upon the reviewers' suggestion, we have added the following in the  
48 conclusion section 6 (line no. 377-380):*

49 *The morphological distinction reported between gullies formed in the bedrock and LDM/glacial deposits  
50 signifies that Martian gullies may have multiple formative mechanisms. We infer that the presence of  
51 mantling material could be one of the key factors in constraining the mechanisms forming Martian gully  
52 systems and that presence of LDM would promote formation of elongated alcoves with perimeter and  
53 relief relatively higher than that of alcoves formed in coarse-grained bedrock substrate.*

54 **Comment 2a.** The authors should be clearer about how they distinguish a gully incised into LDM and a  
55 gully incised into bedrock that is later mantled. You mention in Section 4.1 (second paragraph) that the  
56 gully systems in four craters appear to have incised prior to being mantled. Shouldn't these be in a separate  
57 class rather than being included with the LDM craters?

58 **Comment 2b.** A related question is whether there are any constraints on the depth of mantling material.  
59 One would imagine that a gully eroding into one meter of mantle over bedrock would be morphologically  
60 different from a gully eroding into hundreds of meters of mantle over bedrock.

61 **Response 2a.** *The gully systems formed within LDM are consistent with elongated V-shaped alcoves,*  
62 *polygonized gully banks and adjacent crater wall surfaces, and smoothed gully-fan surfaces. On the*  
63 *other hand, gully systems formed in the bedrock would have alcoves directly cutting into the crater-rim*  
64 *material and may host many boulders, exposing bedrock. The polygonal patterned surface is not evident*  
65 *in these craters. We have used this observational criteria to differentiate between gullies incised into*  
66 *bedrock and LDM.*

67 *Emplacement of mantling material on the crater walls is a cyclic phenomenon, driven primarily by*  
68 *insolation at the Martian poles during the past epochs of higher spin axis obliquity excursions (i.e.*  
69 *obliquity > 35°). Hence, it would be difficult to infer about the presence or absence of LDM for the gullies*  
70 *that currently appear to be mantled. Moreover, potential evidence of elongated V-shaped alcoves,*  
71 *polygonized gully banks and adjacent crater wall surfaces, and smoothed gully-fan surfaces, are all*  
72 *evident in the 4 craters (Raga, Roseau, unnamed crater in Newton basin and unnamed crater-1 in Terra*  
73 *Sirenum) studied in this work. Therefore, we think that we cannot separate the gullies in these 4 craters*  
74 *as a separate class (based on the appearance of the pre-existing mantled gully systems in these craters)*  
75 *and included with the LDM craters.*

76 *In the second paragraph, we intend to infer that among the 24 gullied craters, 4 gullied craters have only*  
77 *LDM and the remaining 20 craters have both LDM and glacial deposits.*

78 *We have revised the second paragraph to clearly bring out the aforementioned aspect. Please see below:*

79 *'4 craters out of 24 craters (i.e. Raga, Roseau, unnamed crater in Newton basin and unnamed crater-1*  
80 *in Terra Sirenum) have gullies that are only influenced by LDM. In these craters, we have found*  
81 *morphological evidence of LDM in the form of polygonized, smooth textured material on the pole-facing*  
82 *walls of the craters. Morphological evidence of VFF is not evident in these craters. In these craters, the*  
83 *gully-alcoves and gully channels appear to have been incised into the polygonized LDM material, and*  
84 *the gully-fan deposits are mantled. A typical example of this can be found in the unnamed crater formed*  
85 *inside the Newton basin (Fig. 4a). Roseau crater, in particular, contains a large number of gully systems*  
86 *whose alcoves and fans are extensively mantled (Fig. 4b). The remaining 20 out of 24 craters contain*  
87 *evidence for gullies that are influenced by both LDM and glacial deposits (Table 1). The base of the....'*

88 *Please refer to line no. 177-184 of the revised version.*

89 **Response 2b.** *In our study, we have not carried out observations to infer the thickness of mantling*  
90 *material. Our study is focused upon inferring whether the morphology and morphometry of gully systems*  
91 *vary in presence or absence of LDM. Therefore, we think, we cannot comment on this aspect right now.*

92 **Comment 3.** “Melton ratio” should be capitalized throughout.

93 **Response 3.** Done. ‘Melton ratio’ has been capitalized at all the places.

94 **Comment 4.** “LDA” is never defined.

95 **Response 4.** Done. We have defined ‘LDA’ as lobate debris apron at its first occurrence (in Table 1) in  
96 the revised manuscript.

97

98

99 **Line comments**

100 **Comment 1.** Line 47: I suggest defining “viscous flow features (VFF)” as an umbrella term for glacial-  
101 type formations ([https://doi.org/10.1007/978-1-4614-9213-9\\_596-1](https://doi.org/10.1007/978-1-4614-9213-9_596-1)). Debris flow deposits could be  
102 considered are “viscous flow features” but presumably are not what you are referring to.

103 **Response 1.** Done. *As suggested, we have rephrased this sentence as follows:*

104 *VFFs are defined as an umbrella term for glacial-type formations covering a broad range of landforms*  
105 *that include lobate debris aprons, concentric crater fill, and lineated valley fills.*

106 *Also, added this reference: Hargitai, H. (2014). Viscous Flow Features (Mars). In: Encyclopedia of*  
107 *Planetary Landforms. Springer, New York, NY. [https://doi.org/10.1007/978-1-4614-9213-9\\_596-1](https://doi.org/10.1007/978-1-4614-9213-9_596-1).*

108 *Please see line no. 48-50 of the revised version.*

109 *Yes, the debris-flow deposits reported in this work are not ‘viscous flow features’.*

110 **Comment 2.** Line 114: Suggest changing “the features listed in 1” to “LDM or glacial features”

111 **Response 2.** Done. *Changed ‘the features listed in 1’ to ‘LDM/glacial deposits’.* Please see line no. 115  
112 *of the revised version.*

113 **Comment 3.** Line 152: “which may eventually influence the morphometric measurements” suggest  
114 changing to “which may have influenced the morphometry”.

115 **Response 3.** Done. Changed 'which may eventually influence the morphometric measurements' to 'which  
116 may have influenced the morphometry'. Please see line no. 152 of the revised version.

117 **Comment 4.** Line 153: "gully fans" should this be "gully systems"?

118 **Response 4.** Done. Changed 'gully fans' to 'gully systems'. Please see line no. 154 of the revised version.

119 **Comment 5.** Line 155: How certain are you that the gullies are incised into LDM material rather than  
120 being incised into bedrock and then later mantled by LDM material? You mention some of the latter in  
121 Section 4.1.

122 **Response 5.** We request the reviewer to please refer to the response to comment no. 2a. We think we  
123 cannot infer about formation of gullies initially into the bedrock and then later it got mantled by the LDM  
124 material.

125 We have revised the section 4.1. Request the reviewer to please see the response to comment no. 2a.

126 **Comment 6.** Line 156: "At first,"-> "First,"

127 **Response 6.** Done. Changed 'at first' to 'First'. Please see line no. 158 of the revised version.

128 **Comment 7.** Line 180: "generation" -> "generations"

129 **Response 7.** This line got deleted during the revision of the manuscript.

130 **Comment 8.** Line 185: "Gullies incised into LDM/VFFs are found to have a distinctive V-shaped cross  
131 section" As written it is unclear if this applies to just the 20 or the 24 craters (including Raga, Roseau,  
132 unnamed crater in Newton basin, and unnamed crater-1 in Terra Sirenum)?

133 **Response 8.** This sentence has been revised as follows:

134 In majority of the gullied craters (except Raga, Roseau and unnamed crater-1 in Terra Sirenum)  
135 influenced by LDM and glacial deposits, gully alcoves are found to have a distinctive V-shaped cross  
136 section in their mid-section, they do not extend up to the crater rim, and gully systems often show multiple  
137 episodes of activity, inferred by the presence of fresh channel incision on the gully-fan surfaces (Fig. 4d-  
138 e).

139 Please see line no. 186-190 of the revised version.

140 **Comment 9.** Line 185: "distinctive V-shaped cross section" You might add a figure showing the  
141 differences in cross sections between a gully incised into LDM/VFF and a gully incised into bedrock.

142 **Response 9.** *We request the reviewer to please see Figure 4d-e (for V-shaped cross-section of gully*  
143 *alcoves incising into LDM/VFF) and Figure 4f (for gullies incising into bedrock). As suggested, we have*  
144 *added reference to these figures in the text on line no. 188 and 281 of the revised manuscript.*

145 **Comment 10.** Line 217: “167 gullies” I suggest adding a column to Table 1 that contains the number of  
146 measured gullies in each crater

147 **Response 10.** *Done. A column has been added to Table 1 to show the number of gullies analysed in each*  
148 *crater.*

149 **Comment 11.** Line 264: “viz. grain size” What is “viz”?

150 **Response 11.** *‘viz.’ is used as a synonym for ‘namely’, ‘that is to say’, ‘to wit’, ‘which is’, or ‘as follows’.*  
151 *For clarity, we have replaced ‘viz.’ with ‘namely’.* Please see line 268 of the revised version of the  
152 *manuscript.*

153 **Comment 12.** Line 289: “V- shape of the incision” this was never really demonstrated in the manuscript

154 **Response 12.** *V-shaped incision has been shown on Figures 4d-e and 7a-d. We request the reviewer to*  
155 *please see these figures. V-shaped incision is marked by arrow and/or labeled on the figure panels. As*  
156 *suggested, we have added reference to these figures in the text on line no. 188 and 281 of the revised*  
157 *manuscript.*

158 **Comment 13.** Line 342: “combinations of Melton ratio” I think that you need to specify the significance  
159 of the Melton ratio here. Why not use some other metric like form factor or elongation ratio on the x-  
160 axis?

161 **Response 13.** *Done. We have added the following on line no. 347-350 of the revised version:*

162 *We have specifically chosen the combinations of Melton ratio with alcove length and fan gradient to infer*  
163 *the Martian gully formative mechanism because they have been widely used in discriminating terrestrial*  
164 *drainage basins and fans prone to flooding from those subject to debris flows, debris floods and floods*  
165 *(e.g. De Scally and Owens, 2004; Wilford et al., 2004).*

166 **Comment 14.** Line 356 “debris-flow like process” What was the fluid source? You mention sublimation  
167 of CO<sub>2</sub> ice in the conclusions but I think you need to elaborate more here.

168 **Response 14.** *Done. We have added the following:*

169 *It is likely that the present-day sublimation of CO<sub>2</sub> ice on Mars provided the necessary flow fluidization*  
170 *for the emplacement of deposits similar to terrestrial debris-flow like deposits (De Haas et al., 2019b).*

171 *Please see line no. 364-366 of the revised version.*

172 **Figure comments**

173 **Comment 1.** Figure 2: Are the examples shown in Figure 2 representative of all of the study craters you  
174 examined? Were there craters where the distinction between bedrock and LDM/glacial was more  
175 ambiguous?

176 *Response 1. Yes, they are representative of all the craters. As such, there were no issues in differentiating*  
177 *between craters influenced by LDM/glacial deposits and bedrock. Gullied craters with LDM could be*  
178 *identified unambiguously based on the evidence of polygonal cracks on the crater walls and gully banks.*  
179 *Glacial deposits were evident in the form of arcuate ridges (at the base of crater wall) and crater floor*  
180 *deposits such as small-scale LDAs. In case of gullies forming within the crater wall bedrock, we have not*  
181 *encountered evidence of polygonal cracks on the wall and/or gully banks, alcoves were having more*  
182 *boulders and appeared to be directly cutting into the crater rim material, and glacial deposits were not*  
183 *evident in these craters.*

184 **Comment 2.** Figure 2d: On line 148 you say that you only selected gully systems that were “not  
185 superimposed by or interfingering with the fans from the neighboring channels” and had “no evidence of  
186 extensive cross-cutting”. This does not appear to be the case for the gullies shown in Figure 2d (see  
187 portion of HiRISE image ESP\_056668\_1345\_RED attached. North is toward the left). You should replace  
188 2d with an example of a bedrock gully that you collected morphometric measurements for (or if you did  
189 collect measurements of the system shown in 2d, revise the text on line 148).

190 *Response 2. Yes, we have selected only those fans that do not superimpose with the fans from the*  
191 *neighboring channels. Additionally, gully channels that exhibit evidence of cross-cutting were not*  
192 *selected for measurements. If in any case the fans superimpose or channels cross-cut, we have carefully*  
193 *demarcated the alcove-channel-fan boundary, to minimize the inaccuracies in the measurements.*

194 *In order to improve the clarity in presentation of the ideas, as suggested by the reviewer, we have revised*  
195 *Figure 2d. The revised Figure 2d shows the portion of the gully system that was selected for measurement.*

196 *Additionally, we have added the following in the section 3.3:*

197 *If in any case the fans superimpose or channels cross-cut, we have carefully demarcated the alcove-*  
198 *channel-fan boundary, to minimize the inaccuracies in the measurements.*

199 *Please see line no. 152-154 of the revised version.*

200 **Comment 3.** Figure 3: Consider changing “Alcove top” to “alcove crest” in left frame for consistency  
201 with text on line 133

202 **Response 3.** Done. As suggested, Figure 3 has been revised. 'Alcove top' is replaced with 'Alcove crest'.

203 **Comment 4.** Figure 4b: Same comment as 2d. The fans appear to partially overlap.

204 **Response 4.** Please refer to our response to comment no. 2. Please note that 'If in any case the fans  
205 superimpose or channels cross-cut, we have carefully demarcated the alcove-channel-fan boundary, to  
206 minimize the inaccuracies in the measurements.'

207 **Comment 5.** Figure 5: I suggest making this figure smaller by reducing the space between the green and  
208 pink boxes in each frame. Also make the order of the figures match the order in Table 2 (e.g., "Melton  
209 ratio" should come after "Fan area" instead of "Alcove relief"). "RCI" is never defined in the text - add  
210 it to "Relative concavity index (RCI)" in Table 2

211 **Response 5.** Done. As suggested by the reviewer, Figure 5 has been revised. The spacing between boxes  
212 has been reduced and the plots are arranged as per their order in Table 2.

213 **Comment 6.** Figure 6: This figure does not add much to the paper. The main finding of the paper (that  
214 gullies formed in bedrock and LDM are morphologically distinct) is presented in Figure 5. It doesn't  
215 really matter for the paper's results which metrics correlate with which other metrics. Furthermore many  
216 of these metrics are related making the correlation (or lack thereof) somewhat meaningless (e.g., length  
217 and area, or length and form factor).

218 **Response 6.** We used the correlation analysis to investigate the relationship between the different  
219 attributes of gully systems formed in LDM/glacial deposits and bedrock. This is an important analysis  
220 because it tells us about the variations in the selected morphometric attributes of the gully systems with  
221 respect to the other. For example, from this analysis we came to know that the perimeter and relief of  
222 alcoves formed in bedrock shows very strong positive correlation with alcove length, but the correlation  
223 was slightly weaker for alcove relief and alcove length in the case of LDM/glacial deposits. Furthermore,  
224 it can be seen that there are relatively less number of morphometric attributes in LDM/glacial deposits  
225 than in bedrock, which shows negative correlation.

226 **Comment 7.** Figure 6: Same comment as Figure 5 - make the order of the figures match the order in  
227 Table 2. I would rotate the labels along the diagonal by 90°. The number of significant figures should be  
228 consistent in (a) and (b) (a is all 2, but b varies). There only needs to be one red-blue scale bar.

229 **Response 7.** As suggested by the reviewer, the correlation matrix plot has been revised. The order of  
230 parameters appearing in the figure matches with Table 2. The number of significant figures is consistent  
231 in both the panels. There is only one scale bar in the revised figure.



232 **Comment 8.** Figure 8: The green triangles and blue circles are very difficult to distinguish from each  
233 other. Use the same pink and green colors as Figure 5. Also I suggest using filled circles/triangles rather  
234 than outlines. What are the dray areas (question mark in second attached figure)?

235 **Response 8.** Done. The colors of the triangles and circles have been changed to green and pink,  
236 respectively. This is consistent with the color of boxes in the box plot shown in Figure 5. We have not  
237 filled the symbols since those prevent seeing the overlap clearly. The gray area shows the realm of the  
238 colluvial, debris-flow, and fluvial fans together. It has been included in the figure caption.

239  
240  
241  
242  
243  
244  
245  
246  
247  
248  
249  
250  
251  
252  
253  
254  
255  
256  
257

258 **Morphologic and Morphometric Differences between Gullies Formed**  
259 **in Different Substrates on Mars: New Insights into the Gully**  
260 **Formation Processes**

261 Rishitosh K. Sinha<sup>1,2</sup>, Dwijesh Ray<sup>1</sup>, Tjalling De Haas<sup>3</sup>, Susan J. Conway<sup>4</sup>, Axel Noblet<sup>4</sup>

262 <sup>1</sup> Physical Research Laboratory, Ahmedabad 380009, Gujarat, India

263 <sup>2</sup> Indian Institute of Technology, Gandhinagar 382355, Gujarat, India

264 <sup>3</sup> Faculty of Geoscience, Universiteit Utrecht, Princetonlaan 8a, 3584 CB Utrecht, the Netherlands

265 <sup>4</sup> Nantes Université, Université d'Angers, Le Mans Université, CNRS UMR 6112 Laboratoire de Planétologie et Géosciences,

266 France

267

268 *Correspondence to:* Rishitosh K. Sinha (rishitosh@prl.res.in)

269 **Abstract.** Martian gullies are kilometer-scale geologically young features with a source alcove, transportation channel, and  
270 depositional fan. On the walls of impact craters, these gullies typically incise into bedrock or surfaces modified by latitude  
271 dependent mantle (LDM; inferred as consisting ice and admixed dust) and glaciation. To better understand the differences in  
272 alcoves and fans of gullies formed in different substrates and infer the flow types that led to their formation, we have analyzed  
273 the morphology and morphometry of 167 gully systems in 29 craters distributed between 30°S and 75°S. Specifically we  
274 measured length, width, gradient, area, relief, and relief ratio of alcove and fan, Melton ratio, relative concavity index, and  
275 perimeter, form factor, elongation ratio and circularity ratio of the alcoves. Our study reveals that alcoves formed in  
276 LDM/glacial deposits are more elongated than the alcoves formed in bedrock, and possess a distinctive V-shaped cross section.  
277 We have found that mean gradient of fans formed by gullies sourced in bedrock is steeper than the mean gradient of fans of  
278 gullies sourced in LDM/glacial deposits. These differences between gullies were found to be statistically significant and  
279 discriminant analysis has confirmed that alcove perimeter, alcove relief and fan gradient are the most important variables for  
280 differentiating gullies according to their source substrates. The comparison between the Melton ratio, alcove length and fan  
281 gradient of Martian and terrestrial gullies reveals that Martian gully systems were likely formed by terrestrial debris-flow like  
282 processes. It is likely that the present-day sublimation of CO<sub>2</sub> ice on Mars provided the adequate flow fluidization for the  
283 formation of deposits akin to terrestrial debris-flow like deposits.

284 **1 Introduction**

285 Gullies are found on steep slopes polewards of about 30° latitude in both hemispheres on Mars and manifest as kilometer-  
286 scale, geologically young features (formed within the last few million years) comprising an alcove, channel, and depositional  
287 fan (Malin and Edgett, 2000; Dickson et al., 2007; Reiss et al., 2004; Schon et al., 2009). Gullies occur in a wide assortment  
288 of settings, varying from the walls and central peaks of craters to walls of valleys, and steep faces of dunes, hills and polar pits

Deleted: melton

Deleted: melton

291 (e.g. Balme et al., 2006; Dickson et al., 2007; Dickson and Head, 2009; Conway et al., 2011, 2015; Harrison et al., 2015). On  
292 the walls of craters, gullies are found to have incised into the (1) surfaces covered by latitude dependent mantle (LDM; e.g.  
293 Mustard et al., 2001; Dickson et al., 2012, 2015), (2) surfaces modified by former episodes of glaciation (Hubbard et al., 2011;  
294 Souness et al., 2012; Souness and Hubbard, 2012; Sinha and Vijayan, 2017), and (3) bedrock (e.g. Johnsson et al., 2014; de  
295 Haas et al., 2019a; Sinha et al., 2020). Detailed investigation of the gullies formed over these different substrates is key to  
296 understanding the intricacies of past processes by which these gullies have formed on Mars (Conway et al., 2015; de Haas et  
297 al., 2019a).

298 A variety of models have been proposed to explain the formation of gullies, which include: (1) dry flows triggered by  
299 sublimation of CO<sub>2</sub> frost (e.g. Cedillo-Flores et al., 2011; Dundas et al., 2012, 2015; Pilorget and Forget, 2016; de Haas et al.,  
300 2019b), (2) debris-flows of an aqueous nature (e.g. Costard et al., 2002; Levy et al., 2010; Conway et al., 2011; Johnsson et  
301 al., 2014; de Haas et al., 2019a; Sinha et al., 2020), and (3) fluvial flows (e.g. Heldmann and Mellon, 2004; Heldmann et al.,  
302 2005; Dickson et al., 2007; Reiss et al., 2011). To better understand the gully formation processes, morphometric investigation  
303 of gullies formed over different substrates needs to be undertaken at a level of detail previously not attempted.

304 The global distribution of gullies shows a spatial correlation with the landforms indicative of glaciation and LDM deposition  
305 on Mars (e.g. Levy et al., 2011; Dickson et al., 2015; Harrison et al., 2015; Conway et al., 2018; de Haas et al., 2019a; Sinha  
306 et al., 2020). With respect to glacial landforms, many gullies have formed into viscous flow features (VFF) and they are found  
307 in the same extent of latitudes (e.g. Arfstrom and Hartmann, 2005; de Haas et al., 2018). VFFs are defined as an umbrella term  
308 for glacial-type formations covering a broad range of landforms that include lobate debris aprons, concentric crater fill, and  
309 lineated valley fills (e.g. Squyres, 1978; Levy et al., 2009; Baker et al., 2010; Hargitai, 2014). Together, they are inferred to  
310 be similar to terrestrial debris-covered glaciers (Conway et al., 2018). With respect to LDM, gullies are mostly found on the  
311 pole-facing slopes of crater walls at lower mid-latitudes (30-45°) (e.g. Balme et al. 2006; Kneissl et al. 2010; Harrison et al.  
312 2015; Conway et al. 2017), wherein, LDM is found to be dissected (e.g. Mustard et al., 2001; Milliken et al., 2003; Head et  
313 al., 2003). In the higher latitudes (>45°), LDM is found to be continuous (e.g. Kreslavsky and Head, 2000), and gullies are  
314 evident at both the pole and equator facing slopes (e.g. Balme et al. 2006; Kneissl et al. 2010; Harrison et al. 2015; Conway et  
315 al. 2017). Gullies formed on the formerly glaciated walls of craters are fed from alcoves that do not extend up to the crater rim,  
316 and appear elongated to V-shaped, implying gully-channel incision into ice-rich, unlithified sediments (e.g. Aston et al., 2011;  
317 de Haas et al., 2019a). The alcoves, channels and fan deposits of gullies formed within craters covered by a smooth drape of  
318 LDM, are usually found to have experienced multiple episodes of LDM covering and subsequent reactivation of some of the  
319 pre-existing channels or formation of fresh channels within the draped LDM deposits (e.g. Dickson et al., 2015; de Haas et al.,  
320 2019a). Additionally, there are gullies that directly emanate from well-defined bedrock alcoves that cut into the crater rim in  
321 the absence of LDM and/or glacial deposits (e.g. Johnsson et al., 2014; de Haas et al., 2019a; Sinha et al., 2020). Gullies  
322 formed in these craters have alcoves with sharply defined crests and spurs, exposing the underlying bedrock, and meter-sized

Deleted: cover

324 boulders are found throughout the gully system (e.g. Johnsson et al., 2014; de Haas et al., 2019a; Sinha et al., 2020). Further,  
325 De Haas et al., 2015a found that the stratigraphy of the fans whose source area was in bedrock were more boulder-rich than  
326 those fans fed by catchments in LDM. The findings in these studies suggest that a more detailed investigation of the  
327 morphology and morphometry of the gullies formed over contrasting substrates is important for improving our understanding  
328 of the formative mechanisms of gullies.

329 In this work, we focus on addressing the following research questions:

330 (1) Do the morphology and morphometry of gully systems formed in different substrates differ (i.e. LDM/glacial deposits and  
331 bedrock)?

332 (2) How do the morphometric characteristics of gullies formed on Mars compare to those formed by a range of processes on  
333 Earth, and what does that tell us about the formative processes of Martian gullies?

334 To parameterize the morphometry we will primarily study long profiles. Previously, only a few studies have analyzed the  
335 morphometric characteristics of the gullies by studying long profiles of gullies (e.g. Yue et al., 2014; Conway et al., 2015; De  
336 Haas et al., 2015a; Hobbs et al., 2015). These studies have focused observations on a part of the gully system and suggested  
337 that the differences in the properties of substrate into which the gullies incise play a significant role in promoting the flows  
338 that led to gully formation. Hence, for a more detailed differentiation of the gully types and interpretation of the dominant flow  
339 type that led to gully formation on Mars, quantification of the morphometric characteristics of the entire gully system is crucial.

## 340 **2 Study sites and datasets**

341 We characterize the morphology and morphometry of gullies in 29 craters distributed over the southern hemisphere between  
342 30° S and 75° S latitude (Fig. 1). These 29 craters are selected based on the availability of publicly released High Resolution  
343 Imaging Science Experiment (HiRISE) stereo-pair based digital terrain model (DTM) or the presence of suitable HiRISE  
344 stereo-pair images to produce a DTM ourselves. The HiRISE stereo-pair images are usually ~0.25 - 0.5 m/pixel (McEwen et  
345 al., 2007), so the DTM post spacing is ~1-2 m with vertical precision in the range of tens of centimeters (Kirk et al., 2008).  
346 Among the 29 gullied craters, publicly released DTMs are available for 25 craters  
347 (<https://www.uahirise.org/hiwish/maps/dtms.jsp> - last accessed 18th September 2021) (Table 1). For the remaining 4 craters,  
348 DTMs are produced with the software packages USGS ISIS and BAE Systems SocetSet (Table 1) (Kirk et al., 2008). We  
349 investigated HiRISE images of these 29 gullied craters for detailed morphological characterization of the substrate into which  
350 the crater wall gullies incise (Table 1).

351

352

353 **Table 1.** Summary of the craters included in this study, their locations, number of gullies investigated from the crater, substrate  
 354 on the crater wall in which gullies have incised, key morphological attributes of the substrate, and IDs of HiRISE imagery and  
 355 DTM used for morphological and morphometric investigation of gullies in these craters.

Deleted: diameter

Crater	Latitude	Longitude	No. of gullies	Substrate	Key morphological attributes	HiRISE ID	HiRISE DTM ID
Artik	34.8° S	131.02° E	<u>2</u>	LDM/glacial deposits	Polygons, V-shaped incisions, arcuate ridges, small-scale lobate debris aprons (LDAs) on the floor	ESP_020740_1450	DTEEC_012459_1450_012314_1450_A01
Asimov	47.53° S	4.41° E	<u>4</u>	LDM/glacial deposits	Polygons, V-shaped incisions, mantled alcoves/channels/fans, arcuate ridges, small-scale LDAs inside valleys	ESP_012912_1320	DTEEC_012912_1320_012767_1320_A01
Bunnik	38.07° S	142.07° W	<u>8</u>	LDM/glacial deposits	Polygons, V-shaped incisions, mantled alcoves/channels/fans, arcuate ridges	ESP_047044_1420	DTEEC_002659_1420_002514_1420_U01
Corozal	38.78° S	159.48° E	<u>6</u>	LDM/glacial deposits	Polygons, mantled alcoves/channels/fans, arcuate ridges, small-scale LDAs on the floor	PSP_006261_1410	DTEEC_006261_1410_014093_1410_A01
Dechu	42.23° S	158° W	<u>8</u>	LDM/glacial deposits	Polygons, mantled alcoves/channels/fans, arcuate ridges, small-scale LDAs on the floor	PSP_006866_1375	DTEED_023546_1375_023612_1375_A01
Dunkassa	37.46° S	137.06° W	<u>5</u>	LDM/glacial deposits	Polygons, V-shaped incisions, mantled alcoves/channels/fans, arcuate ridges, small-scale LDAs on the floor	ESP_032011_1425	DTEEC_039488_1420_039343_1420_A01
Hale	35.7° S	36.4° W	<u>8</u>	LDM/glacial deposits	Polygons, V-shaped incisions, mantled alcoves/channels/fans, talus slope deposits	PSP_003209_1445	DTEEC_002932_1445_003209_1445_A01
Langtang	38.13° S	135.95° W	<u>5</u>	LDM/glacial deposits	Polygons, V-shaped incisions, mantled alcoves/channels/fans, arcuate ridges, small-scale LDAs on the floor	ESP_030099_1415	DTEEC_024099_1415_023809_1415_U01

Formatted Table

Moni	46.97° S	18.79° E	<u>5</u>	LDM/glacial deposits	Partly infilled alcoves, mantled fan surfaces, arcuate ridges	ESP_056862_1325	DTEEC_007110_1325_006820_1325_A01
Nybyen	37.03° S	16.66° W	<u>8</u>	LDM/glacial deposits	Polygons, mantled alcoves/channels/fans, arcuate ridges	ESP_059448_1425	DTEEC_006663_1425_011436_1425_A01
Palikir	41.56° S	157.87° W	<u>5</u>	LDM/glacial deposits	Polygons, V-shaped incisions, mantled alcoves/channels/fans, arcuate ridges, small-scale LDAs on the floor	ESP_057462_1380	DTEEC_005943_1380_011428_1380_A01
Penticton	38.38° S	96.8° E	<u>7</u>	LDM/glacial deposits	Polygons, V-shaped incisions, mantled alcoves/channels/fans, arcuate ridges, small-scale LDAs on the floor	ESP_029062_1415	DTEEC_001714_1415_001846_1415_U01
Selevac	37.37° S	131.07° W	<u>8</u>	LDM/glacial deposits	Polygons, mantled alcoves/channels/fans, small-scale flows on the floor	ESP_045158_1425	DTEEC_003252_1425_003674_1425_A01
Raga	48.1° S	117.57° W	<u>4</u>	LDM	Polygons, mantled alcoves/channels/fans	ESP_041017_1315	DTEEC_014011_1315_014288_1315_A01
Roseau	41.7° S	150.6° E	<u>1</u>	LDM	Polygons, mantled alcoves/channels/fans	ESP_024115_1380 / ESP_011509_1380	ESP_024115_1380_ESP_011509_1380*
Taltal	39.5° S	125.8° W	<u>7</u>	LDM/glacial deposits	Polygons, V-shaped incisions, mantled alcoves/channels/fans, arcuate ridges, small-scale LDAs on the floor	ESP_037074_1400 / ESP_031259_1400	ESP_037074_1400_ESP_031259_1400*
Talu	40.34° S	20.11° E	<u>7</u>	LDM/glacial deposits	Polygons, V-shaped incisions, mantled alcoves/channels/fans, arcuate ridges, small-scale LDAs on the floor	ESP_011817_1395	DTEEC_011817_1395_011672_1395_O01
Triolet	37.08° S	168.02° W	<u>4</u>	LDM/glacial deposits	Polygons, V-shaped incisions, mantled alcoves/channels/fans, arcuate ridges, small-scale LDAs on the floor	ESP_047190_1425	DTEEC_023586_1425_024008_1425_A01
Unnamed crater	32.31° S	118.55° E	<u>4</u>	LDM/glacial deposits	Polygons, mantled alcoves/channels/fans	PSP_006869_1475	DTEEC_021914_1475_022336_1475_U01

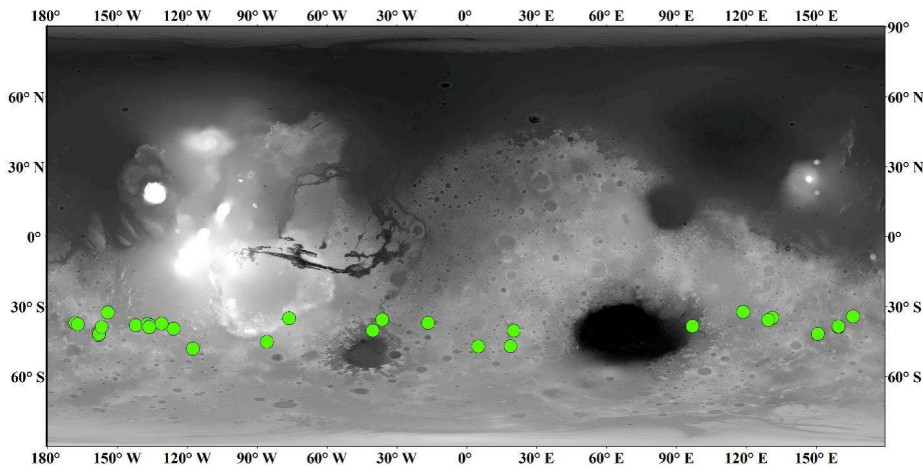
					s, arcuate ridges, small-scale LDAs on the floor		
Unnamed crater in the Argyre basin	40.3° S	40.4° W	<u>6</u>	LDM/glacial deposits	Polygons, mantled alcoves/channels/fans, arcuate ridges, small-scale LDAs on the floor	ESP_032047_1395	DTEEC_012795_1395_013507_1395_A01
Unnamed crater in the Newton basin	38.8° S	156.8° W	<u>5</u>	LDM	Polygons, V-shaped incisions, mantled alcoves/channels/fans	PSP_002686_1410	DTEEC_002620_1410_002686_1410_A01
Unnamed crater north of Corozal crater	38.53° S	159.44° E	<u>5</u>	LDM/glacial deposits	Polygons, mantled alcoves/channels/fans, small-scale LDAs on the floor	ESP_020884_1410	DTEEC_020884_1410_020950_1410_A01
Unnamed crater-1 in the Terra Sirenum	32.55° S	154.11° W	<u>2</u>	LDM	Mantled alcoves/channels/fans	PSP_007380_1470	DTEEC_010597_1470_007380_1470_U01
Unnamed crater-2 in the Terra Sirenum	38.88° S	136.36° W	<u>6</u>	LDM/glacial deposits	Polygons, V-shaped incisions, mantled alcoves/channels/fans, arcuate ridges, small-scale LDAs on the floor	ESP_020407_1410	DTEEC_022108_1410_022385_1410_A01
Istok	45.1° S	85.82° W	<u>8</u>	Bedrock	Alcove cut directly into the original crater-wall material, clasts embedded into fresh deposits on fan	ESP_056668_1345	DTEEC_040607_1345_040251_1345_A01
Galap	37.66° S	167.07° W	<u>8</u>	Bedrock	Alcove cut directly into the original crater-wall material, clasts embedded into fresh deposits on fan	ESP_059770_1420	DTEEC_048983_1420_048693_1420_U01
Gasa	35.73° S	129.4° E	<u>7</u>	Bedrock	Alcove cut directly into the original crater-wall material, clasts embedded into fresh deposits on fan	ESP_057491_1440	DTEEC_021584_1440_022217_1440_A01
Los	35.08° S	76.23° W	<u>7</u>	Bedrock	Alcove cut directly into the original crater-wall material,	ESP_020774_1445 / ESP_050127_1445	ESP_020774_1445_ESP_050127_1445*

					clasts embedded into fresh deposits on fan		
Unnamed crater-3 in the Terra Sirenum	34.27° S	165.71° E	<u>7</u>	Bedrock	Alcove cut directly into the original crater-wall material, clasts embedded into fresh deposits on fan	ESP_049261_1455 / ESP_049828_1455	ESP_049261_1455_ ESP_049828_1455*

357

358 (\*) DTMs are produced with the software packages USGS ISIS and BAE Systems SocetSet.

359



360 Figure 1: Locations of craters analyzed in this study (green circles). Background: Mars Orbiter Laser Altimeter gridded data, where  
 361 white is high elevation and black is low elevation, credit MOLA Science Team/NASA/JPL.

362

### 363 3 Approach

#### 364 3.1 Identification of substrate

365 The substrate into which the gullies have incised is identified based on the following criteria:

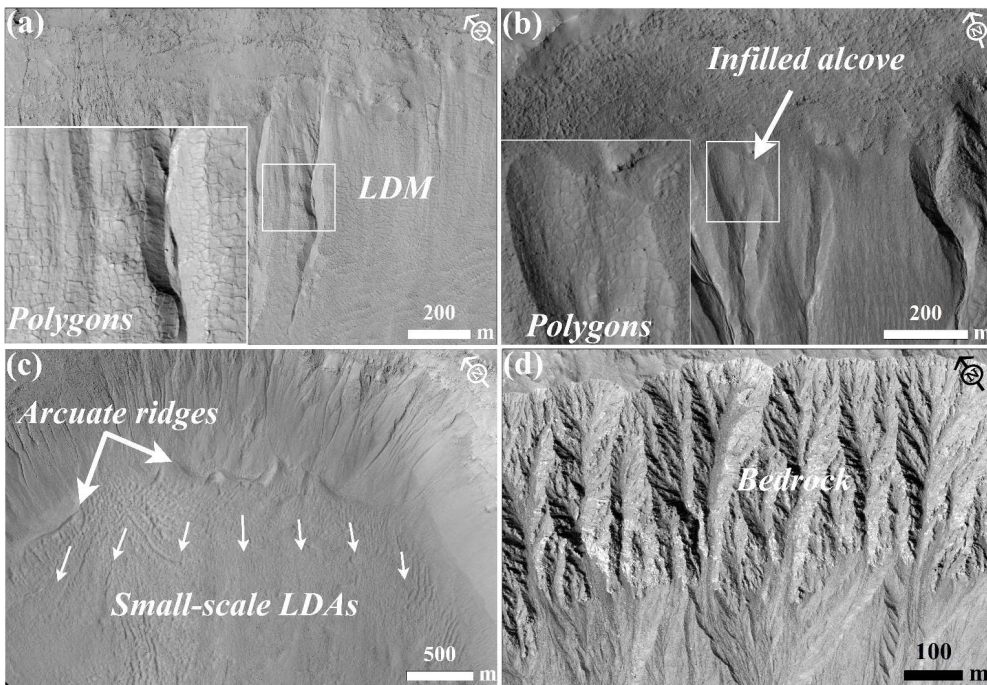
- 366 1. LDM/glacial deposits: Any crater whose gullies incise walls that appear to be softened by the drape of smooth mantling  
 367 material with polygonal cracks is inferred to have LDM as the substrate within which gullies have incised (e.g. Mustard et al.,



368 2001; Kreslavsky and Head, 2002; Levy et al., 2009a; Conway et al., 2018; de Haas et al., 2019a) (Fig. 2a). The alcoves on  
 369 the walls of these craters may be partially to completely filled by LDM, and in some cases, polygonized LDM materials may  
 370 be seen covering the alcove walls (e.g. Christensen, 2003; Conway et al., 2018; de Haas et al., 2019a). These infilled alcoves  
 371 on the crater walls are not the alcoves of gullies formed within the LDM substrate; instead, they represent the alcoves that were  
 372 formed prior to the LDM emplacement epoch. Additionally, gullied craters that show evidence in the form of arcuate ridges at  
 373 the foot of the walls and VFFs that cover part or the entire crater floor are inferred to have been modified by one or multiple  
 374 episodes of glaciation (e.g. Arfstrom and Hartmann, 2005; Head et al., 2010; Milliken et al., 2003; Hubbard et al., 2011). These  
 375 craters host gullies that are often partially or fully covered by LDM deposits.

376 2. Bedrock: Craters where the features listed in LDM/glacial deposits are absent and where rocky material is visible extending  
 377 downwards from the crater rim. This rocky material usually outcrops as spurs and can be layered or massive. The slopes can  
 378 be smooth or covered with boulders, with concentrations of boulders at the slope toe.

Deleted: 1



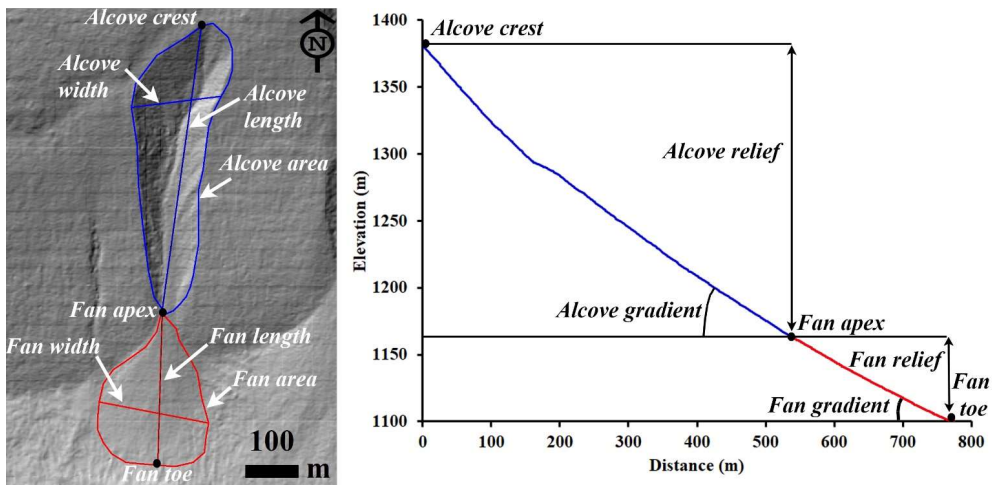
379

381 **Figure 2:** Examples of morphological evidence used to identify LDM, glacial deposits, and bedrock. (a) Smooth mantling material  
 382 inferred as LDM draped on the wall of Talu crater on the basis of polygonal cracks formed in the material. The bigger box is an  
 383 expanded view of the polygons seen over the region outlined by the smaller box. (HiRISE image ESP\_011817\_1395). (b) An infilled  
 384 alcove on the wall of an unnamed crater-2 in the Terra Sirenum. Evidence of polygons in the infilled material suggests presence of  
 385 LDM deposits draped on the wall. The region shown in smaller box is expanded in the bigger box to show evidence of the polygons.  
 386 (HiRISE image ESP\_020407\_1410). (c) Glaciation inferred in the Corozal crater on the basis of arcuate ridges formed at the foot of  
 387 the crater wall and small-scale LDAs on the crater floor. Arrows indicate the downslope flow of LDAs on the floor. (HiRISE image  
 388 PSP\_006261\_1410). (d) Exposed fractured bedrock identified on the walls of Istok crater within which alcoves have incised. (HiRISE  
 389 image ESP\_056668\_1345). HiRISE image credit: NASA/JPL /University of Arizona.

390

### 391 3.2 Morphometric variables

392 The measurements we made of each gully system include alcove area, alcove perimeter, alcove length, alcove width, alcove  
 393 gradient, fan area, fan length, fan width, and fan gradient (Fig. 3). In total, we derived 18 morphometric variables to  
 394 characterize each gully fan and its alcove. The morphometric variables are classified into geometry, relief, gradient, and  
 395 dimensionless variables and they are calculated with established mathematical equations shown in Table 2. For the gradient  
 396 measurement using the DTM, the topographic profile from (1) crest of the alcove to the apex of the fan was extracted for the  
 397 alcove, and (2) apex to foot of the fan was extracted for the fan.



398

399 **Figure 3:** Examples of morphometric variables estimated in this work. Left panel: HiRISE DTM (Id:  
 400 DTEEC\_002659\_1420\_002514\_1420) based hillshade. HiRISE DTM credit: NASA/JPL /University of Arizona. Right panel:

401 Topographic profile: blue profile represents the topography of gully alcove from alcove top to fan apex and red profile represents  
 402 the profile of gully fan from fan apex to fan toe.

403

404

405 **Table 2.** Set of morphometric variables extracted from the studied gully systems and their formulas and/or description of  
 406 method.

Morphometric variable	Formula and/or description of method	References
Alcove length and width	Measured in km	Tomczyk, 2021
Alcove area	Measured in km <sup>2</sup>	Tomczyk, 2021
Fan length and width	Measured in km	Tomczyk, 2021
Fan area	Measured in km <sup>2</sup>	Tomczyk, 2021
Melton ratio	(Alcove relief)/(Alcove area <sup>0.5</sup> )	Melton, 1957
Relative concavity index (RCI)	Concavity Index/(maximum relief between the uppermost and lowermost points along the gully fan profile/2). Concavity Index is estimated as $\sum (H_i^* - H_i) / N$ , where $H_i^*$ is the elevation along the straight line, $H_i$ is the elevation along the gully fan profile, $N$ is the total number of measurement points.	Langbein, 1964; Phillips and Lutz, 2008
Alcove gradient	Measured in (°)	Tomczyk, 2021
Fan gradient	Measured in (°)	Tomczyk, 2021
Alcove relief	Measured in km	Tomczyk, 2021
Fan relief	Measured in km	Tomczyk, 2021
Relief ratio (alcove and fan)	Alcove/fan relief divided by the length of the alcove/fan	Schumm, 1956a, b
Perimeter	Measured in km	Schumm, 1956a, b
Form factor	Alcove area divided by the square of the length of the alcove	Horton, 1932
Elongation ratio	Diameter of a circle of the same area as the alcove divided by the maximum alcove length	Schumm, 1956a, b
Circularity ratio	Alcove area divided by the area of the circle having the same perimeter as the alcove perimeter	Miller, 1953

Formatted Table

407

### 408 3.3 Gully system selection for morphometric measurements

409 We have selected only those gully systems for morphometric measurements in which: (i) the depositional fan from an alcove-  
 410 channel system is not superimposed by or interfingering with the fans from the neighboring channels, (ii) there is clear  
 411 association between the primary channel emanating from the alcove that extends downslope and then deposit its respective  
 412 fan, (iii) no evidence of extensive cross-cutting is seen with the neighboring channels on the walls, (iv) no evidence of extensive  
 413 mantling by dust/aeolian deposits is apparent, and (v) no evidence of channel/fan superposition on any topographic obstacle  
 414 on the walls or the floor of the crater is apparent, which may have influenced the morphometry. If in any case the fans

Deleted: eventually influence the morphometric measurements

416 ~~superimpose or channels cross-cut, we have carefully demarcated the alcove-channel-fan boundary, to minimize the~~  
417 ~~inaccuracies in the measurements.~~ Note that the selection of the gully ~~systems~~ was also constrained by the coverage of HiRISE  
418 DTM that was used for morphometric analysis.

Deleted: fans

### 419 3.4 Statistical analysis of morphometric variables

420 We have two groups of gullies in our study: (1) gullies whose source area is incised into LDM/glacial deposits and (2) gullies  
421 whose source area is incised into the bedrock. ~~First, for both the groups we have calculated descriptive statistics for each of~~  
422 the morphometric variables shown in Table 2. The significance of the difference between the values of each of the  
423 morphometric variables calculated for each group was tested using a Student's t-test. To apply t-tests, we have transformed  
424 the morphometric variables to remove skewness by taking their natural logarithm. Correlation analysis has been used to  
425 investigate the correlation between the selected morphometric attributes of alcoves and fans. We infer strong positive  
426 correlations between variables if the correlation coefficient value is more than 0.7 and strong negative correlations if the value  
427 is less than -0.7. Very strong positive correlation between variables is inferred if the correlation coefficient is  $\geq 0.9$ . Further,  
428 we used canonical discriminant analysis (CDA) to determine morphometric variables that provide the most discrimination  
429 between the groups of gullies. In CDA, functions are generated according to the number of groups, until a number equal to  $n -$   
430 1 functions is reached ( $n$  is the number of groups) (Conway et al., 2015). For the two groups of gullies in our study, there is  
431 going to be a function for which there is a standardised canonical discriminant function coefficient associated with the  
432 morphometric variable. The higher the magnitude of this coefficient for a particular morphometric variable, the higher the role  
433 of that variable in separating the groups of gullies. Standardisation was done by dividing each value for a given variable by  
434 the maximum value.

Deleted: At f

## 435 4 Results

### 436 4.1 Morphology of gully systems

437 Out of the 29 gullied craters analysed in this work, we have found that there are 24 craters influenced by LDM and VFFs. The  
438 remaining 5 craters have gullies incised into the exposed underlying bedrock on the wall of the crater. Below we describe the  
439 substrates identified in the studied craters and then compare the morphology of the gullies formed into those substrates.

440 ~~4 craters out of 24 craters (i.e. Raga, Roseau, unnamed crater in Newton basin and unnamed crater-1 in Terra Sirenum) have~~  
441 ~~gullies that are only influenced by LDM. In these craters, we have found morphological evidence of LDM in the form of~~  
442 ~~polygonized, smooth textured material on the pole-facing walls of the craters.~~ Morphological evidence of VFF is not evident  
443 in these craters. In these craters, the gully-alcoves ~~and gully channels appear to have been incised into the polygonized LDM~~  
444 ~~material,~~ and the gully-fan deposits are ~~mantled~~. A typical example of this can be found in the unnamed crater formed inside  
445 the Newton basin (Fig. 4a). Roseau crater, in particular, contains a large number of gully systems whose alcoves and fans are

Deleted: We found morphological evidence of LDM in the form of polygonized, smooth textured material on the pole-facing walls of 4 craters namely

Deleted: both

Deleted: covered by a smooth drape of polygonized LDM material

Deleted: pre-existing

454 extensively mantled (Fig. 4b). The remaining 20 out of 24 craters contain evidence for gullies that are influenced by both LDM  
455 and glacial deposits (Table 1). The base of the pole-facing walls and the floor of the craters within which the gully systems  
456 have formed host linear-to-sinuuous arcuate ridges and VFFs, respectively. Typical examples of VFFs can be found in Corozal,  
457 Talu, unnamed craters in Terra Sirenum and Argyre basin, Langtang, Dechu and Dunkassa craters (Fig. 4c). In majority of the  
458 gullied craters (except Raga, Roseau and unnamed crater-1 in Terra Sirenum) influenced by LDM and glacial deposits, gully  
459 alcoves are found to have a distinctive V-shaped cross section in their mid-section (Figures 4d and 4e), they do not extend up

**Deleted:** Additionally, younger generation of gullies are visible that have incised within the LDM.

**Deleted:** specifically incised LDM as opposed to LDM that infills pre-existing alcoves and gullies, and

**Deleted:** VFFs

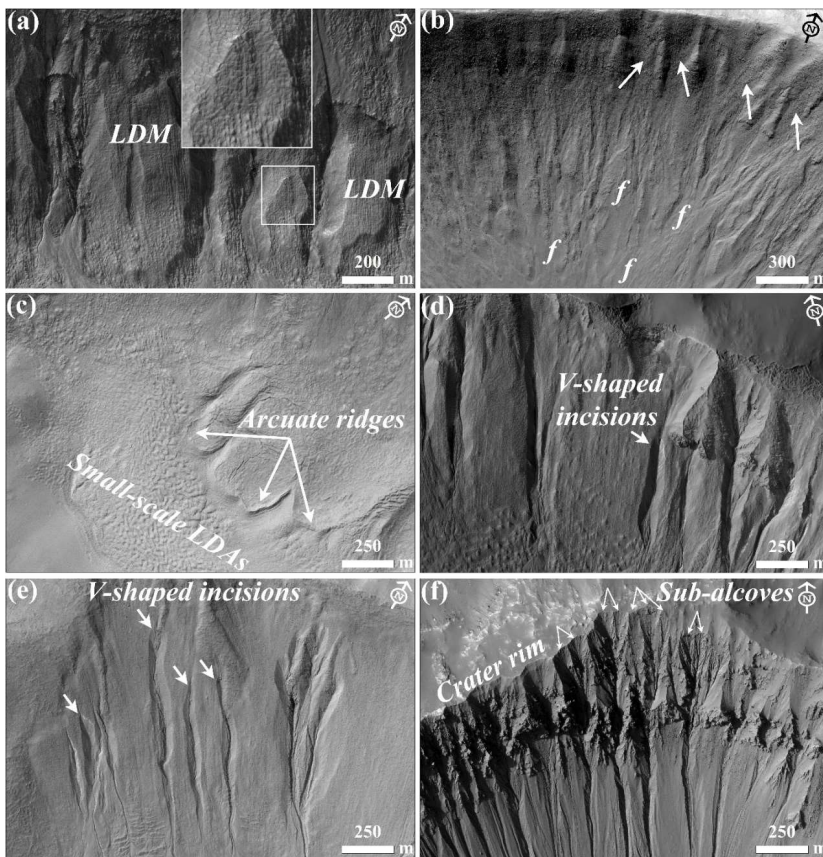
**Deleted:** Gullies

**Deleted:** incised into LDM/VFFs

467 to the crater rim, and gully systems often show multiple episodes of activity, inferred by the presence of fresh channel incision  
468 on the gully-fan surfaces (Fig. 4d-e).

469 Istok, Galap, Gasa, Los, and an unnamed crater in the Terra Sirenum contain gully systems on the pole-facing walls that are  
470 not associated with LDM and VFFs (Table 1). The alcoves inside these craters have a crenulated shape and appear to have  
471 formed by headward erosion into the bedrock of the crater rim (Fig. 4f). These craters have formed large gully systems on  
472 their pole-facing walls, with brecciated alcoves, comprising of multiple sub-alcoves and hosting many clasts/boulders (Fig.  
473 4f).

474  
475  
476  
477  
478  
479  
480  
481  
482  
483  
484  
485  
486  
487  
488  
489  
490



491 **Figure 4:** (a) LDM draped on the wall of an unnamed crater in the Newton basin. The inset shows details of the polygonal texture of  
492 the LDM. (HiRISE image PSP\_002686\_1410). (b) Infilled alcoves (arrows) and mantled fan surfaces (marked by letter 'f') on the  
493 wall of Roseau crater. (HiRISE image ESP\_024115\_1380). (c) Arcuate ridges at the foot of the crater wall and small-scale LDAs on  
494 the floor in Langtang crater. (HiRISE image ESP\_030099\_1415). (d) V-shaped incisions on the LDM draped walls of Taltal (HiRISE  
495 image ESP\_037074\_1400) and (e) Langtang crater (HiRISE image ESP\_030099\_1415). (f) Alcoves formed in Los crater by headward  
496 erosion into the crater rim. Individual alcoves formed in bedrock have multiple sub-alcoves. (HiRISE image ESP\_020774\_1445).

497

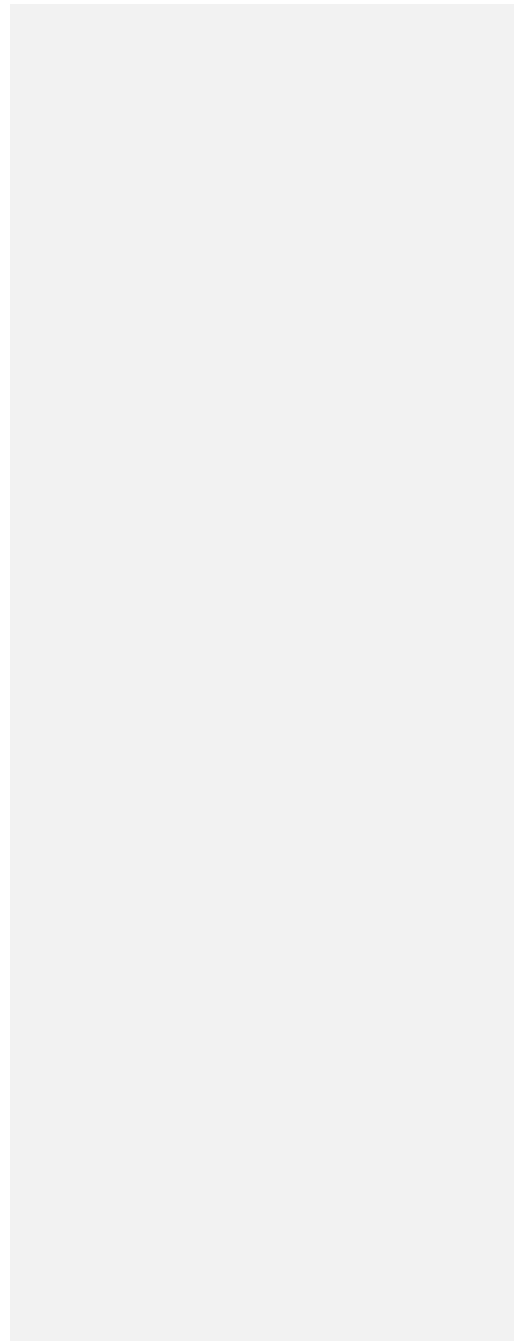
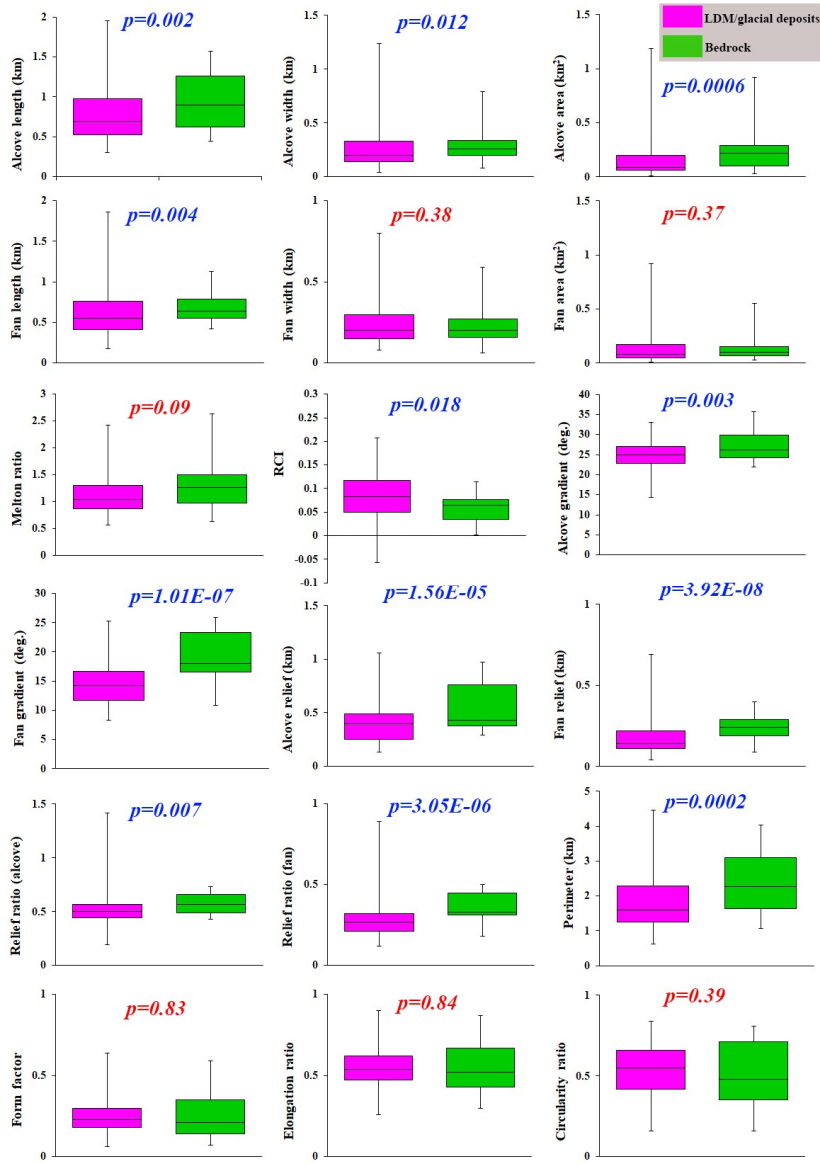
#### 498 4.2 Morphometry of gully systems

499 Based on the criteria summarized in section 3.3, we have studied 167 gullies across 29 craters for calculation of morphometric  
500 variables. 130 gullies are formed within LDM/glacial deposits, and 37 gullies are formed within the bedrock. The results of  
501 morphometric calculations are summarized for visual comparison as a boxplot (Fig. 5).

502 The results of the Student's t-test indicates that all of the morphometric variables in Table 2, except fan width, fan area, Melton  
503 ratio, form factor, elongation ratio, and circularity ratio, differ significantly between LDM/glacial deposits and bedrock (Fig.  
504 5). Compared to the mean gradient of gully-fans formed in LDM/glacial deposits, bedrock gully-fans are steeper and possess  
505 a higher relief ratio. The interquartile range of length, relief, and perimeter of alcoves formed in bedrock are also higher than  
506 the interquartile range of similar variables in LDM/glacial deposits, but the alcoves in LDM/glacial deposits possess much  
507 higher values of length, relief, and perimeter (Fig. 5).

508

Deleted: melton



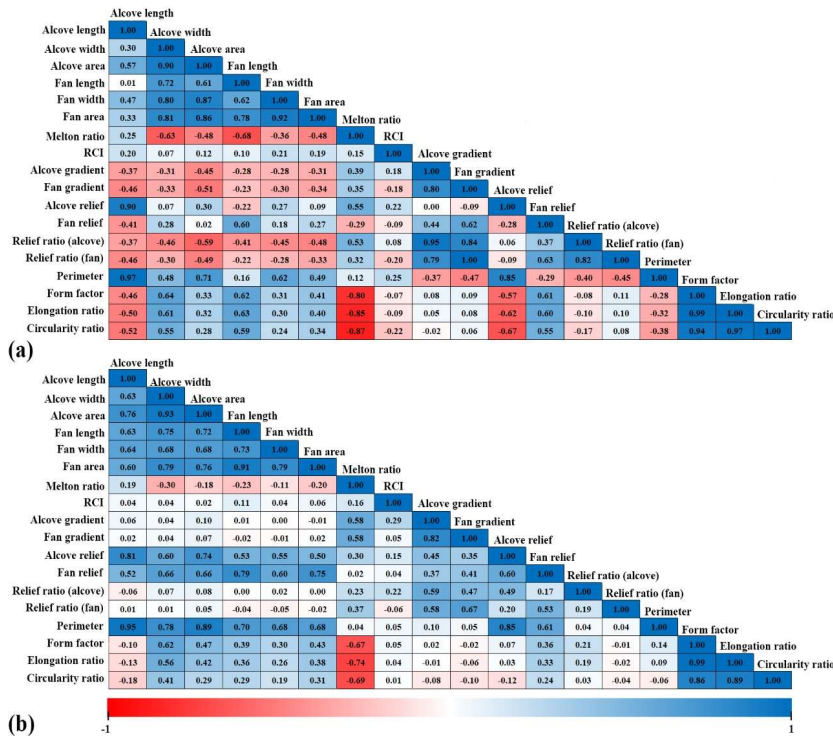


512 **Figure 5: Boxplots showing the range of values of alcove/fan geometry, relief, gradient, and dimensionless variables of gullies incised**  
 513 **into LDM/glacial deposits (pink) and bedrock (green). P-values on the plots represent the results of the student's t-tests for testing**  
 514 **the significance of difference in means of the morphometric variables between gully systems formed on LDM/Glacial deposits and**  
 515 **bedrock. P-values in blue correspond to significant difference (with respect to a p-value of 0.05) and those in red are non-significant.**

516

517 Correlations between morphometric attributes of alcoves and fans formed in bedrock and LDM/glacial deposits are  
 518 summarized in Fig. 6. For bedrock, there are strong positive correlations between 12 pairs of morphometric variables and  
 519 strong negative correlations between 3 pairs of morphometric variables. For LDM/glacial deposits, there are strong positive  
 520 correlations between 18 pairs of morphometric variables and strong negative correlations between 3 pairs of morphometric  
 521 variables. Very strong positive correlations are found between 9 pairs of morphometric variables for bedrock and between 4  
 522 pairs of morphometric variables for LDM/glacial deposits.

523



524 **Figure 6: Correlations between morphometric attributes of alcoves and fans formed in (a) bedrock and (b) LDM/glacial deposits.**  
525 **Higher the value of the correlation coefficient, higher is the strength of the correlation.**

526

527 The canonical discriminant analysis reveals that the following morphometric variables best distinguish between the gully  
528 systems formed in LDM/glacial deposits and bedrock, in descending order of importance: alcove perimeter, alcove relief, fan  
529 gradient, fan relief, fan length, relief ratio (alcove), alcove width, relief ratio (fan), alcove gradient, alcove area, alcove length,  
530 and relative concavity index (Table 3). The alcove perimeter is most important in discriminating among the gully systems  
531 formed within LDM/glacial deposits and bedrock, and the next two most important variables are alcove relief and fan gradient.  
532 Alcove relief and fan gradient have 4/5 and 1/3 the weight of alcove perimeter, respectively. The remaining variables such as  
533 fan relief, fan length, relief ratio (alcove), alcove width, and relief ratio (fan) have nearly 1/5 the weight of alcove perimeter  
534 or greater (but less than 1/3) discriminatory power in separating between the gullies formed in LDM/glacial deposits and  
535 bedrock. The variables with the smallest magnitude, alcove gradient, alcove area, alcove length and relative concavity index,  
536 have less than 1/10 the weight of the most important variable in separating the gully systems.

537 **Table 3.** Standardised canonical discriminant function coefficients (F1) that best separate gully systems formed on  
538 LDM/Glacial deposits and bedrock.

Variable	F1
Perimeter	3.552
Alcove relief	-2.828
Fan gradient	1.278
Fan length	-1.06
Fan relief	1.06
Relief ratio (alcove)	0.971
Alcove width	-0.692
Relief ratio (fan)	-0.665
Alcove gradient	-0.331
Alcove area	-0.319
Alcove length	0.23
Relative concavity index	-0.182

539

## 540 5 Discussions

### 541 5.1 Unique morphology and morphometry of gully systems in different substrates

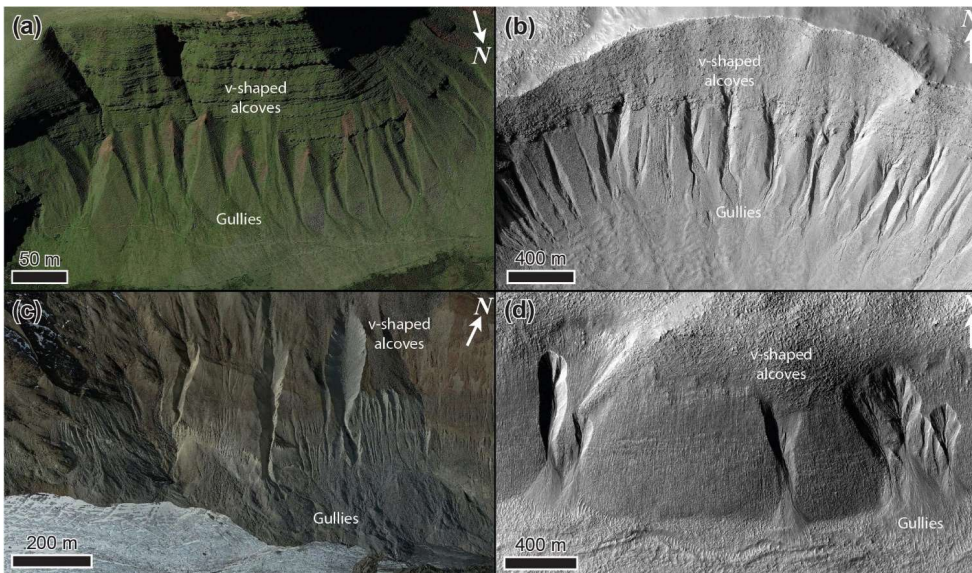
542 We have found that the gully systems formed in LDM/glacial deposits and bedrock can, using discriminatory analysis, be  
543 distinguished from one another in terms of perimeter and relief of alcoves (Table 3). Additionally, we have found statistically  
544 significant difference between the perimeter and relief of alcoves formed in LDM/glacial deposits and bedrock (Fig. 5). It is  
545 likely that these differences in the perimeter and relief of alcoves formed within morphologically distinct substrates could be  
546 due to the integral nature of the surface material within which the alcoves have formed. In other words, it is possible that the  
547 differences in the physical properties of the sediments (~~namely~~ grain size, compactness etc.) within which alcoves have formed  
548 played a key role in erosion of the substrate leading to differences in their morphometric variables. Below we elaborate on the  
549 uniqueness of the substrates within which alcoves have formed, and discuss further the relationships between the morphometric  
550 variables of the morphologically distinct gully systems.

551 On Mars, VFFs contain high purity glacial ice with a debris cover (Sharp, 1973; Squyres, 1978, 1979; Squyres and Carr, 1986;  
552 Holt et al 2008, Plaut et al 2009, Petersen et al. 2018). Their surfaces have been interpreted to be comprised of finer, reworked  
553 debris derived from sublimation of the underlying ice (Mangold, 2003; Levy et al., 2009a; Morgan et al., 2009). The smooth,  
554 meters thick draping unit on the walls of formerly glaciated craters has been suggested to be derived from the atmosphere as a  
555 layer of dust-rich ice primarily constituting of fine-grained materials (Kreslavsky and Head, 2000; Mustard et al., 2001). The  
556 fine-grained materials are loosely-packed, unconsolidated materials exhibiting low thermal inertia values (Mellon et al., 2000;  
557 Putzig et al., 2005). Typically, gullies formed within this substrate display a smooth surface texture, wherein, evidence of  
558 individual clasts or meter-scale boulders is not resolvable in HiRISE images, substantiating the dominant component of fine-  
559 grained materials within the LDM (e.g., Levy et al., 2010; de Haas et al., 2015a). Additionally, it has been found that alcoves  
560 incised into the LDM always have a distinctive V-shaped cross section in their mid-section (Figures 4d and 4e), which when  
561 compared with similar-scaled systems on Earth also corresponds to the presence of loose sediments constituting the LDM  
562 (Conway et al., 2018). The alcoves with V-shaped cross sections are found to be elongated, likely indicating incision within  
563 ice-rich unlithified sediments (Aston et al., 2011). In the studied craters, we have found that gullies incised into LDM/glacial  
564 deposits are having an elongated, V-shaped cross section in their mid-section (Fig. 4). We propose that the presence of fine-  
565 grained, loosely packed, unconsolidated materials within LDM/glacial deposits has facilitated formation of elongated alcoves  
566 with perimeter and relief relatively higher than that of alcoves formed in coarse-grained bedrock substrate. This is consistent  
567 with the previous studies suggesting that gullies eroding into LDM/glacial deposits have elongated catchments, whereas gullies  
568 eroding into the bedrock have more amphitheater-shaped catchments (Levy et al., 2009b). For this reason, the estimated length  
569 of alcoves formed in LDM/glacial deposits is found to be relative higher than that of alcoves formed in bedrock (Fig. 5).  
570 Furthermore, statistical analysis has revealed a significant difference between the length of alcoves formed in LDM/glacial  
571 deposits and bedrock (Fig. 5). Additionally, the presence of finer-grained sediments in LDM/glacial deposits is the likely cause

Deleted: viz.

573 of the V-shape of the incision of alcoves investigated in this study (Aston et al., 2011). On Earth, V-shaped incisions through  
574 glacial ice-rich moraines have been observed to have occurred during the paraglacial phase of glacial retreat (Bennett et al.,  
575 2000; Ewertowski and Tomczyk, 2015) (Fig. 7). The paraglacial phase refers to a terrestrial post-glacial period that represents  
576 the response of changing environment to deglaciation (Bennett et al., 2000; Ewertowski and Tomczyk, 2015).

577



578

579 **Figure 7: Gullies forming in glacial sediments in deglaciated terrain in the (a) Brecon Beacons, Wales, UK on Earth (Google Earth**  
580 **coordinates: 51°52'59.11"N, 3°43'33.26"W), (b) Talu crater ([https://www.uahirise.org/ESP\\_011817\\_1395](https://www.uahirise.org/ESP_011817_1395)) on Mars, (c)**  
581 **Hintereisferner, Austria (Google Earth coordinates: 46°48'54.25"N, 10°47'8.18"E), on Earth, and (d) Bunnik crater**  
582 **([https://www.uahirise.org/ESP\\_047044\\_1420](https://www.uahirise.org/ESP_047044_1420)) on Mars. HiRISE image credit: NASA/JPL-Caltech/University of Arizona.**

583

584 The next most important difference between these two types of gullies is the mean gradient of gully fans. At the foot of the  
585 fans, mean gradient of the fans influenced by LDM/glacial deposits is  $<15^\circ$  for 61% of the studied fans. For bedrock, 84% of  
586 the studied fans have a mean gradient  $>15^\circ$  at the foot of the fans. Hence, gully-fans formed in bedrock are emplaced at a  
587 relatively steeper gradient than the fans formed from gullies in LDM/glacial deposits. We propose that the nature of the material

588 mobilized can explain this difference, with the finer-grained sediments characteristic of the LDM/glacial type gullies being  
589 easier to mobilise and being entrained to lower slope angles, than the coarser sediments found within the bedrock type gullies.

## 590 **5.2 Evaluation of the gully formation process**

591 On Earth, alcove-fan systems can roughly be subdivided in flood-dominated, debris-flow dominated, and colluvial systems.  
592 Following the terminology of De Haas et al., (2015b) and Tomczyk (2021), we define these systems as follows:

593 1) Flood-dominated systems: These are systems dominated by fluid-gravity flows, i.e., water floods, hyperconcentrated floods,  
594 and debris floods. The fans of such systems are commonly referred to as fluvial or alluvial fans (e.g., Ryder, 1971; Blair and  
595 McPherson, 1994; Hartley et al., 2005).

596 2) Debris-flow dominated systems: These are systems dominated by sediment-gravity flows, i.e., debris flows, mud flows.  
597 Irrespective of their radial extent and depositional gradients, the fans aggraded by these systems can be commonly called  
598 debris-flow fans or debris fans (Blikra and Nemeč, 1998; de Scally et al., 2010).

599 3) Colluvial systems: These are systems dominated by rock-gravity and sediment-gravity flows, with their dominant activity  
600 relating to rockfalls, grain flows, and snow avalanches (in periglacial and alpine settings). Debris flows typically constitute  
601 only a relatively minor component of geomorphic processes in such systems. The fans of these systems are also commonly  
602 known as colluvial cones or talus cones (Siewert et al., 2012; De Haas et al., 2015b).

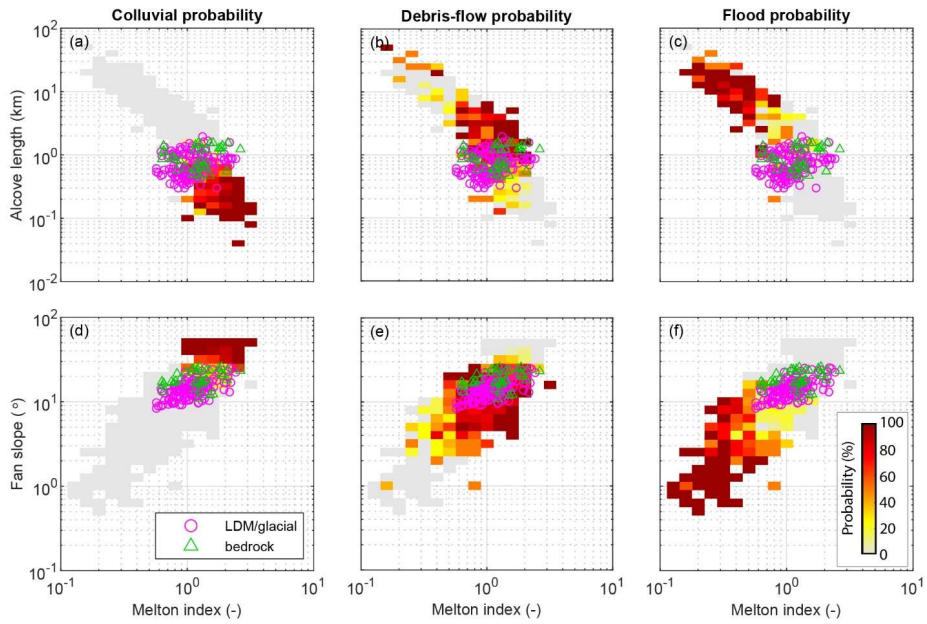
603 Although these systems may be dominated by one type of geomorphic process, it is important to stress that other processes  
604 may also occur. For example, on Earth water floods are not uncommon on many debris-flow dominated systems, while debris-  
605 flow deposits are commonly recognized on colluvial cones.

606

607

608

609



610

611 **Figure 8: Comparison of combinations of Melton ratio with Alcove length and Fan gradient. The probability heat maps**  
612 **are based on previously published data – see text for references. The Martian gully systems formed in LDM/glacial**  
613 **deposits and bedrock are found to be in the debris-flow regime on Earth. The gray area shows the realm of the colluvial,**  
614 **debris-flow, and fluvial fans together.**

615

616 To compare the morphometric characteristics of the Martian gully systems to terrestrial systems, we have compiled  
617 morphometric data of alcoves and fans across several continents, mountain ranges, climate zones, and process types on Earth.  
618 This dataset includes published data from the Himalayas, Ladakh, India (Stolle et al., 2013), the tropical Andes, Columbia  
619 (Arango et al., 2021), Spitsbergen, Svalbard (Tomczyk, 2021), British Columbia, Canada (Kostaschuk, 1986; Jackson et al.,  
620 1987; and newly presented data), the southern Carpathians, Romania (Ilinca et al., 2021), the Southern Alps, New Zealand (De  
621 Scally and Owens, 2004; De Scally et al., 2010), the North Cascade Foothills, USA, the European Alps (including Switzerland,  
622 Italy, France, and Austria), and the Pyrenees (from multiple authors compiled by Bertrand et al., 2013). The dataset comprises  
623 information from colluvial, debris-flow, and flood (also including debris flood) dominated systems. In total, it contains 231

624 colluvial systems, 749 debris-flow dominated systems, and 369 flood-dominated systems. In total, data were compiled for  
625 1349 systems, although not all information was available for all systems, with data availability ranging from 729 sites for  
626 alcove length to all 1349 systems for Melton index and process type. Based on this data we have made a heatmap of the  
627 probability of flood, debris-flow, or colluvially-dominated conditions for combinations of Melton ratio with alcove length and  
628 fan gradient, to which we compare the Martian gullies (Fig. 8). We have specifically chosen the combinations of Melton ratio  
629 with alcove length and fan gradient to infer the Martian gully formative mechanism because they have been widely used in  
630 discriminating terrestrial drainage basins and fans prone to flooding from those subject to debris flows, debris floods and floods  
631 (e.g. De Scally and Owens, 2004; Wilford et al., 2004). We have found that the Martian gullies are indeed in the debris-flow  
632 regime on Earth. Moreover, they are closer to the transition to the smaller and steeper colluvial cones than to transition to  
633 flood-dominated fans. As expected, bedrock systems in Fig. 8d-e are closer to the colluvial systems than the LDM systems.

634

635 According to the previous reports of debris-flow like deposits found in Martian gullies (e.g. Johnsson et al., 2014; Sinha et al.,  
636 2019, 2020), the morphological attributes of debris-flow like deposits typically include overlapping tongue-shaped lobes with  
637 embedded clasts, channels with medial deposits, and channels with clearly defined lateral levees. Although it is still not clear  
638 whether the formation of these deposits in gullies are from sublimation of CO<sub>2</sub> ice or due to meltwater generation. De Haas et  
639 al., (2019b) showed that CO<sub>2</sub> sublimation may lead to flow fluidization on Mars in a manner similar to fluidization by water  
640 in terrestrial debris flows; a concept supported by the recent finding of lobate deposits and boulder-rich levee formation during  
641 the present-day in Istok crater (Table 1) (Dundas et al., 2019). The formation of these morphologically similar deposits during  
642 the present-day is attributed to sublimating CO<sub>2</sub> frost, which likely produces the necessary fluidization likely by gas generated  
643 from entrained CO<sub>2</sub> frost (Dundas et al., 2019). On the basis of these recent reports (De Haas et al., 2019b; Dundas et al., 2019)  
644 and based on our own findings in this study, we argue that a debris-flow like process similar to those operated in the terrestrial  
645 gully systems has likely dominated the flow types that lead to gully formation on Mars. It is likely that the present-day  
646 sublimation of CO<sub>2</sub> ice on Mars provided the necessary flow fluidization for the emplacement of deposits similar to terrestrial  
647 debris-flow like deposits (De Haas et al., 2019b).

## 648 6 Conclusions

649 This paper compares morphological and morphometric characteristics of gully alcoves and associated fans formed in  
650 LDM/glacial deposits and bedrock over walls of 29 craters between 30° S and 75° S latitudes. 5 craters out of 29 have alcoves-  
651 fans formed within the bedrock and remaining 24 craters have alcoves-fans formed within LDM/glacial deposits. From our  
652 analysis of 167 gullies, we posit that gully systems formed in LDM/glacial deposits and bedrock differ from one another using  
653 the following lines of evidence:

Formatted: Font: Not Bold

Formatted: Font: Not Bold

654 • Alcoves formed in LDM/glacial deposits are more elongated than the alcoves formed in bedrock, and possess a distinctive  
655 V-shaped cross section.

656 • The mean gradient of gully-fans formed in bedrock is steeper than the mean gradient of fans formed from gullies in  
657 LDM/glacial deposits.

658 The morphological distinction reported between gullies formed in the bedrock and LDM/glacial deposits signifies that Martian  
659 gullies may have multiple formative mechanisms. We infer that the presence of mantling material could be one of the key  
660 factors in constraining the mechanisms forming Martian gully systems and that presence of LDM would promote formation  
661 of elongated alcoves with perimeter and relief relatively higher than that of alcoves formed in coarse-grained bedrock substrate.

662 Based on the combinations of Melton ratio with alcove length and fan gradient, we suggest that the gully systems studied in  
663 this work were likely dominated by terrestrial debris-flow like processes during their formation. This is consistent with the  
664 findings reported in previous studies that showed evidence of formation of deposits morphologically similar to terrestrial  
665 debris-flow like deposits, both in the past and during the present-day (e.g., Johnsson et al., 2014; Dundas et al., 2019). The  
666 present-day sublimation of CO<sub>2</sub> ice on Mars is envisaged to provide the necessary flow fluidization for the emplacement of  
667 deposits similar to debris-flow like deposits on Earth (De Haas et al., 2019b).

#### 668 **7 Author contribution**

669 RKS, TDH and SJC conceptualized this work. The methodology was developed by RKS, TDH and SJC. Data curation and  
670 formal analyses were performed by RKS. TDH and AN also contributed in collection of datasets used in this work. RKS, DR,  
671 TDH and SJC contributed to the interpretation of the data and results. RKS wrote the original draft of this paper, which was  
672 reviewed and edited by all authors.

#### 673 **8 Conflict of interest**

674 SJC is a Guest Editor of this special issue (Planetary landscapes, landforms, and their analogues) of ESurfD and on the editorial  
675 board for ESurf. The peer-review process was guided by an independent editor, and the authors have also no other competing  
676 interests to declare.

#### 677 **9 Acknowledgements**

678 We are grateful and thank both the anonymous reviewers for thorough assessment of our manuscript and for providing us  
679 constructive comments and suggestions. Thanks to the Editor (Heather Viles) and Associate Editor (Frances E. G. Butcher) at  
680 Earth Surface Dynamics for the editorial handling of the manuscript. We would like to thank the HiRISE team for their work  
681 to produce the images and digital elevation models used in this study, it would have been impossible without them. RKS and  
682 DR acknowledge the financial support by the Indian Space Research Organisation, Department of Space, Government of India.



683 SJC and AN are grateful for the financial support from Région Pays de la Loire, project étoiles montantes METAFLOWS  
684 (convention N° 2019-14294) and also the financial support of CNES in support of their HiRISE work. TdH was supported by  
685 the Netherlands Organisation for Scientific Research (NWO) (grant 016.Veni.192.001). We acknowledge the efforts of team  
686 MUTED to develop an online tool (<http://muted.wwu.de/>) for quick identification of the spatial and multi-temporal coverage  
687 of planetary image data from Mars. All the planetary datasets used in this work are available for free download at the PDS  
688 Geosciences Node Mars Orbital Data Explorer (ODE) (<https://ode.rsl.wustl.edu/mars/>) and <https://www.uahirise.org/>. The  
689 newly-generated DTMs can be downloaded from [https://figshare.com/articles/dataset/Self\\_generated\\_DEMs/21717164](https://figshare.com/articles/dataset/Self_generated_DEMs/21717164).  
690 The measurement datasets can be downloaded from  
691 [https://figshare.com/articles/dataset/Measurement\\_data\\_of\\_gully\\_systems\\_in\\_the\\_southern\\_mid\\_latitudes\\_of\\_Mars/](https://figshare.com/articles/dataset/Measurement_data_of_gully_systems_in_the_southern_mid_latitudes_of_Mars/21717182)  
692 [21717182](https://figshare.com/articles/dataset/Measurement_data_of_gully_systems_in_the_southern_mid_latitudes_of_Mars/21717182). This work is a part of the PhD work of Rishitosh K. Sinha. Director PRL, Head of Planetary Science Division,  
693 PRL, Head of Planetary Remote Sensing Section, PRL, and Director IIT Gandhinagar are gratefully acknowledged for constant  
694 encouragement during the work.

#### 695 **References**

- 696 Arango, M. I., Aristizábal, E., & Gómez, F.: Morphometrical analysis of torrential flows-prone catchments in tropical and  
697 mountainous terrain of the Colombian Andes by machine learning techniques, *Natural Hazards*, 105(1), 983-1012, doi:  
698 <https://doi.org/10.1007/s11069-020-04346-5>, 2021.
- 699 Arfstrom, J. & Hartmann, W.K.: Martian flow features, moraine-like ridges, and gullies: terrestrial analogs and  
700 interrelationships, *Icarus*, 174, 321-335, doi: <https://doi.org/10.1016/j.icarus.2004.05.026>, 2005.
- 701 Aston, A., Conway, S. & Balme, M.: Identifying Martian Gully Evolution. In: Balme, M.R., Bargery, A.S., Gallagher, C.J. &  
702 Gupta, S. (eds) *Martian Geomorphology*, Geological Society, London, Special Publications, 356, 151-169, doi:  
703 <https://doi.org/10.1144/SP356.9>, 2011.
- 704 Balme, M., Mangold, N. Et Al.: Orientation and distribution of recent gullies in the southern hemisphere of Mars: observations  
705 from High Resolution Stereo Camera/Mars Express (HRSC/MEX) and Mars Orbiter Camera/Mars Global Surveyor  
706 (MOC/MGS) data, *J. Geophys. Res.: Planets*, 111, E05001, doi: <https://doi.org/10.1029/2005JE002607>, 2006.
- 707 Bertrand, M., Liébault, F., & Piégay, H.: Debris-flow susceptibility of upland catchments, *Natural Hazards*, 67(2), 497-511,  
708 doi: <https://doi.org/10.1007/s11069-013-0575-4>, 2013.
- 709 Blair, T.C. & McPherson, J.G.: Processes and forms of alluvial fans. In: PARSONS, A. & ABRAHAM, A. (eds)  
710 *Geomorphology of Desert Environments*, Springer, Dordrecht, The Netherlands, 413-467, doi: [https://doi.org/10.1007/978-1-](https://doi.org/10.1007/978-1-4020-5719-9_14)  
711 [4020-5719-9\\_14](https://doi.org/10.1007/978-1-4020-5719-9_14), 2009.

712 Blair, T.C.: Sedimentology of the debris-flow-dominated Warm Spring Canyon alluvial fan, Death Valley, California,  
713 *Sedimentology* 46 (5), 941–965, doi: <https://doi.org/10.1046/j.1365-3091.1999.00260.x>, 1999.

714 Blikra, L.H., Nemeč, W.: Postglacial colluvium in western Norway: depositional processes, facies and palaeoclimatic record.  
715 *Sedimentology* 45 (5), 909–960, doi: <https://doi.org/10.1046/j.1365-3091.1998.00200.x>, 1998.

716 Cedillo-Flores, Y., Treiman, A.H., Lasue, J. & Clifford, S.M.: CO<sub>2</sub> gas fluidization in the initiation and formation of Martian  
717 polar gullies, *Geophys. Res. Letters*, 38, L21202 doi: <https://doi.org/10.1029/2011GL049403>, 2011.

718 Christensen, P.R.: Formation of recent Martian gullies through melting of extensive water-rich snow deposits, *Nature*, 422,  
719 45–48, doi: <https://doi.org/10.1038/nature01436>, 2003.

720 Conway, S. J., Butcher, F. E., de Haas, T., Deijns, A. A., Grindrod, P. M., & Davis, J. M.: Glacial and gully erosion on Mars:  
721 A terrestrial perspective, *Geomorphology*, 318, 26-57, doi: <https://doi.org/10.1016/j.geomorph.2018.05.019>, 2018.

722 Conway, S.J. & Balme, M.R.: Decameter thick remnant glacial ice deposits on Mars, *Geophys. Res. Letters*, 41, 5402–5409,  
723 doi: <https://doi.org/10.1002/2014GL060314>, 2014.

724 Conway, S.J., Balme, M.R., Kreslavsky, M.A., Murray, J.B. & Towner, M.C.: The comparison of topographic long profiles  
725 of gullies on Earth to gullies on Mars: a signal of water on Mars. *Icarus*, 253, 189–204, doi:  
726 <https://doi.org/10.1016/j.icarus.2015.03.009>, 2015.

727 Conway, S.J., Balme, M.R., Murray, J.B., Towner, M.C., Okubo, C.H. & Grindrod, P.M.: The indication of Martian gully  
728 formation processes by slope–area analysis, In: Balme, M.R., Bargery, A.S., Gallagher, C.J. & Gupta, S. (eds) *Martian*  
729 *Geomorphology*, Geological Society, London, Special Publications, 356, 171–201, doi: <https://doi.org/10.1144/SP356.10>,  
730 2011.

731 Conway, S.J., Harrison, T.N., Soare, R.J., Britton, A.W. & Steele, L.J.: New slope-normalized global gully density and  
732 orientation maps for Mars, In: Conway, S.J., Carrivick, J.L., Carling, P.A., De Haas, T. & Harrison, T.N. (eds) *Martian Gullies*  
733 *and their Earth Analogues*, Geol. Soc. Lond. Spec. Publ. 467. First published online November 27, 2017, doi:  
734 <https://doi.org/10.1144/SP467.3>, 2017.

735 Costard, F., Forget, F., Mangold, N. & Peulvast, J.P.: Formation of recent Martian debris flows by melting of near-surface  
736 ground ice at high obliquity, *Science*, 295, 110–113, doi: [10.1126/science.1066](https://doi.org/10.1126/science.1066), 2002.

737 Crosta, G.B., Frattini, P.: Controls on modern alluvial fan processes in the central Alps, northern Italy, *Earth Surf. Proc. Land*.  
738 29 (3), 267–293, doi: <https://doi.org/10.1002/esp.1009>, 2004.

739 de Haas, T., Conway, S.J., Butcher, F.E.G., Levy, J.S., Grindrod, P.M., Balme, M.R., Goudge, T.A.: Time will tell: temporal  
740 evolution of Martian gullies and paleoclimatic implications, *Geol. Soc. Lond. Spec. Publ.* 467, doi:  
741 <https://doi.org/10.1144/SP467.1>, 2019a.

742 de Haas, T., McArdell, B. W., Conway, S. J., McElwaine, J. N., Kleinhans, M. G., Salese, F., & Grindrod, P. M.: Initiation  
743 and flow conditions of contemporary flows in Martian gullies, *J. Geophys. Res.: Planets*, 124(8), 2246-2271, doi:  
744 <https://doi.org/10.1029/2018JE005899>, 2019b.

745 de Haas, T., Hauber, E. & Kleinhans, M.G. 2013. Local late Amazonian boulder breakdown and denudation rate on Mars,  
746 *Geophys. Res. Letters*, 40, 3527–3531, doi: <https://doi.org/10.1002/grl.50726>, 2013.

747 de Haas, T., Ventra, D., Hauber, E., Conway, S.J. & Kleinhans, M.G.: Sedimentological analyses of Martian gullies: the  
748 subsurface as the key to the surface, *Icarus*, 258, 92–108, doi: <https://doi.org/10.1016/j.icarus.2015.06.017>, 2015a.

749 de Haas, T., Kleinhans, M. G., Carbonneau, P. E., Rubensdotter, L., & Hauber, E.: Surface morphology of fans in the high-  
750 Arctic periglacial environment of Svalbard: Controls and processes, *Earth-Science Reviews*, 146, 163-182, doi:  
751 <https://doi.org/10.1016/j.earscirev.2015.04.004>, 2015b.

752 de Scally, F. A., & Owens, I. F.: Morphometric controls and geomorphic responses on fans in the Southern Alps, New Zealand,  
753 *Earth Surface Processes and Landforms: The Journal of the British Geomorphological Research Group*, 29(3), 311-322, doi:  
754 <https://doi.org/10.1002/esp.1022>, 2004.

755 De Scally, F.A., Owens, I.F., Louis, J.: Controls on fan depositional processes in the schist ranges of the Southern Alps, New  
756 Zealand, and implications for debris-flow hazard assessment, *Geomorphology* 122 (1–2), 99–116, doi:  
757 <https://doi.org/10.1016/j.geomorph.2010.06.002>, 2010.

758 Dickson, J.L. & Head, J.W.: The formation and evolution of youthful gullies on Mars: gullies as the latestage phase of Mars  
759 most recent ice age, *Icarus*, 204, 63–86, doi: <https://doi.org/10.1016/j.icarus.2009.06.018>, 2009.

760 Dickson, J.L. et al.: Recent climate cycles on Mars: Stratigraphic relationships between multiple generations of gullies and the  
761 latitude dependent mantle, *Icarus* 252, 83–94, doi: <http://dx.doi.org/10.1016/j.icarus.2014.12.035>, 2015.

762 Dickson, J.L., Head, J.W., Fassett, C.I.: Patterns of accumulation and flow of ice in the mid-latitudes of Mars during the  
763 Amazonian, *Icarus* 219, 723–732, doi: <http://dx.doi.org/10.1016/j.icarus.2012.03.010>, 2012.

764 Dickson, J.L., Head, J.W., Kreslavsky, M.: Martian gullies in the southern midlatitudes of Mars: Evidence for climate-  
765 controlled formation of young fluvial features based upon local and global topography, *Icarus* 188, 315–323, doi:  
766 <https://doi.org/10.1016/j.icarus.2006.11.020>, 2007.

767 Dundas, C. M., McEwen, A. S., Diniega, S., Hansen, C. J., Byrne, S., & McElwaine, J. N.: The formation of gullies on Mars  
768 today, *Geol. Soc. Lond. Spec. Publ.* 467, 67-94, doi: <https://doi.org/10.1144/SP46>, 2019.

769 Dundas, C.M., Diniega, S., Hansen, C.J., Byrne, S., McEwen, A.S.: Seasonal activity and morphological changes in martian  
770 gullies, *Icarus* 220:124–143, doi: <https://doi.org/10.1016/j.icarus.2012.04.005>, 2012.

771 Dundas, C.M., Diniega, S., McEwen, A.S.: Long-term monitoring of Martian gully formation and evolution with  
772 MRO/HiRISE, *Icarus* 251:244–263, doi: <https://doi.org/10.1016/j.icarus.2014.05.013>, 2015.

773 [Hargitai, H. \(2014\). Viscous Flow Features \(Mars\). In: Encyclopedia of Planetary Landforms. Springer, New York, NY.](https://doi.org/10.1007/978-1-4614-9213-9_596-1)  
774 [https://doi.org/10.1007/978-1-4614-9213-9\\_596-1](https://doi.org/10.1007/978-1-4614-9213-9_596-1)

775 Harrison, T.N., Osinski, G.R., Tornabene, L.L., Jones, E.: Global documentation of gullies with the Mars reconnaissance  
776 orbiter context camera and implications for their formation, *Icarus* 252:236–254, doi:  
777 <https://doi.org/10.1016/j.icarus.2015.01.022>, 2015.

778 Hartley, A.J., Mather, A.E., Jolley, E., Turner, P.: Climatic controls on alluvial-fan activity, Coastal Cordillera, northern Chile.  
779 In: Harvey, A.M., Mather, A.E., Stokes, M. (Eds.), *Alluvial Fans: Geomorphology, Sedimentology, Dynamics*. *Geol. Soc.*  
780 *Lond. Spec. Publ.* 251, 95-115, doi: <https://doi.org/10.1144/GSL.SP.2005.251.01>, 2005.

781 Head, J.W., Marchant, D.R., Dickson, J.L., Kress, A.M., Baker, D.M.: Northern midlatitude glaciation in the Late Amazonian  
782 period of Mars: criteria for the recognition of debris-covered glacier and valley glacier landsystem deposits, *Earth Planet. Sci.*  
783 *Lett.* 294:306–320, doi: <https://doi.org/10.1016/j.epsl.2009.06.041>, 2010.

784 HELDMANN, J.L. & MELLON, M.T.: Observations of Martian gullies and constraints on potential formation mechanisms,  
785 *Icarus*, 168, 285–304, doi: <https://doi.org/10.1016/j.icarus.2003.11.024>, 2004.

786 Heldmann, J.L. et al.: Formation of martian gullies by the action of liquid water flowing under current martian environmental  
787 conditions, *J. Geophys. Res. Planets* 110, doi: <http://dx.doi.org/10.1029/2004JE002261>, 2005.

788 Hobbs, S.W., Paull, D.J., Clark, J.D.A.: A comparison of semiarid and subhumid terrestrial gullies with gullies on Mars:  
789 Implications for martian gully erosion, *Geomorphology* 204, 344–365, doi: <http://dx.doi.org/10.1016/j.geomorph.2013.08.018>,  
790 2014.

791 Hobbs, S.W., Paull, D.J. and Clarke, J.D.A.: Analysis of regional gullies within Noachis Terra, Mars: A complex relationship  
792 between slope, surface material and aspect, *Icarus*, 250, 308-331, doi: <https://doi.org/10.1016/j.icarus.2014.12.011>, 2015.

793 Hubbard, B., Milliken, R.E., Kargel, J.S., Limaye, A. & Souness, C.: Geomorphological characterisation and interpretation of  
794 a mid-latitude glacier-like form: Hellas Planitia, Mars, *Icarus*, 211, 330–346, doi: <https://doi.org/10.1016/j.icarus.2010.10.021>,  
795 2011.

796 Ilinca, V.: Using morphometrics to distinguish between debris flow, debris flood and flood (Southern Carpathians, Romania),  
797 *Catena*, 197, 104982, doi: <https://doi.org/10.1016/j.catena.2020.104982>, 2021.

798 Jackson LE, Kostaschuk RA, MacDonald GM: Identification of debris flow hazard on alluvial fans in the Canadian Rocky  
799 Mountains, In: Costa JE, Wieczorek GF (eds) *Debris flows/avalanches: process, recognition, and mitigation*. *Rev Eng Geol*  
800 vol. VII. *Geol. Soc. Am*, doi: <https://doi.org/10.1130/REG7-p115>, 1987.

801 Johnsson, A. et al.: Evidence for very recent melt-water and debris flow activity in gullies in a young mid-latitude crater on  
802 Mars, *Icarus* 235, 37–54, doi: <http://dx.doi.org/10.1016/j.icarus.2014.03.005>, 2014.

803 Kirk, R.L., Howington-Kraus, E., Rosiek, M.R., Anderson, J.A., Archinal, B.A., Becker, K.J., Cook, D.A., Galuszka, D.M.,  
804 Geissler, P.E., Hare, T.M., Holmberg, I.M., Keszthelyi, L.P., Redding, B.L., Delamere, W.A., Gallagher, D., Chapel, J.D.,  
805 Eliason, E.M., King, R., McEwen, A.S.: Ultrahigh resolution topographic mapping of Mars with MRO HiRISE stereo images:  
806 meter-scale slopes of candidate Phoenix landing sites, *J. Geophys. Res. Planets* 113, doi:  
807 <https://doi.org/10.1029/2007JE003000>, 2008.

808 Kostaschuk, R.A., Macdonald, G.M., Putnam, P.E.: Depositional process and alluvial fan-drainage basin morphometric  
809 relationships near Banff, Alberta, Canada, *Earth Surf. Proc. Land.* 11 (5), 471–484, doi:  
810 <https://doi.org/10.1002/esp.3290110502>, 1986.

811 Kreslavsky, M.A.: Slope steepness of channels and aprons: Implications for origin of martian gullies. Workshop Martian  
812 Gullies, Workshop on Martian Gullies 2008. Abs.#1301, 2008.

813 Kreslavsky, M.A., Head, J.W.: Mars: nature and evolution of young latitudedependent water-ice-rich mantle, *Geophys. Res.*  
814 *Lett.* 29, doi: <https://doi.org/10.1029/2002GL015392>, 2002.

815 Langbein, W. B.: Profiles of rivers of uniform discharge, *U.S. Geol. Surv. Prof. Pap.*, 501-B, 119– 122, doi:  
816 <https://doi.org/10.1086/627653>, 1964.

817 Lanza, N. L., Meyer, G. A., Okubo, C. H., Newsom, H. E., & Wiens, R. C.: Evidence for debris flow gully formation initiated  
818 by shallow subsurface water on Mars, *Icarus*, 205(1), 103-112, doi: <https://doi.org/10.1016/j.icarus.2009.04.014>, 2010.

819 Levy, J.S. et al.: Identification of gully debris flow deposits in Protonilus Mensae, Mars: Characterization of a water-bearing,  
820 energetic gully-forming process, *Earth Planet. Sci. Lett. Mars Express after 6 Years in Orbit: Mars Geology from Three-*  
821 *Dimensional Mapping by the High Resolution Stereo Camera (HRSC) Experiment 294*, 368–377, doi:  
822 <https://doi.org/10.1016/j.epsl.2009.08.002>, 2010b.

823 Levy, J.S., Head, J., Marchant, D.: Thermal contraction crack polygons on Mars: classification, distribution, and climate  
824 implications from HiRISE observations, *J. Geophys. Res. Planets* 114, 01007, doi: <https://doi.org/10.1029/2008JE003273>,  
825 2009a.

826 Levy, J. S., Head, J. W., Marchant, D. R., Dickson, J. L., & Morgan, G. A.: Geologically recent gully–polygon relationships  
827 on Mars: Insights from the Antarctic Dry Valleys on the roles of permafrost, microclimates, and water sources for surface  
828 flow, *Icarus*, 201(1), 113-126, doi: <https://doi.org/10.1016/j.icarus.2008.12.043>, 2009b.

829 Levy, J.S., Head, J.W., Marchant, D.R.: Gullies, polygons and mantles in Martian permafrost environments: cold desert  
830 landforms and sedimentary processes during recent Martian geological history, *Geol. Soc. Lond. Spec. Publ.* 354, 167–182,  
831 doi: <https://doi.org/10.1144/SP354.10>, 2011.

832 Malin, M.C., Edgett, K.S.: Evidence for recent groundwater seepage and surface runoff on Mars. *Science* 288:2330–2335, doi:  
833 <https://doi.org/10.1126/science.288.5475.2330>, 2000.

834 Mcewen, A.S., Eliason, E.M. et al.: Mars reconnaissance orbiter’s High Resolution Imaging Science Experiment (HiRISE), *J.*  
835 *Geophys. Res.: Planets*, 112, E05S02, doi: <https://doi.org/10.1029/2005JE002605>, 2007.

836 Melton, M.A.: An analysis of the relation among elements of climate, surface properties and geomorphology, Office of Nav.  
837 Res. Dept. Geol. Columbia Univ, NY. Tech. Rep. 11, 1975.

838 Milliken, R.E., Mustard, J.F., Goldsby, D.L.: Viscous flow features on the surface of Mars: observations from high-resolution  
839 Mars Orbiter Camera (MOC) images, *J. Geophys. Res.* 108, doi: <https://doi.org/10.1029/2002JE002005>, 2003.

840 Mustard, J.F., Cooper, C.D., Rifkin, M.K.: Evidence for recent climate change on Mars from the identification of youthful  
841 near-surface ground ice, *Nature* 412:411–414, doi: <https://doi.org/10.1038/35086515>, 2001.

842 Phillips, J.D., Lutz, J.D.: Profile convexities in bedrock and alluvial streams, *Geomorphology* 102, 554–566, doi:  
843 <https://doi.org/10.1016/j.geomorph.2008.05.042>, 2008.

844 Pilorget, C. & Forget: Formation of gullies on mars by debris flows triggered by CO2 sublimation, *Nature Geoscience*, 9, 65–  
845 69, doi: <https://doi.org/10.1038/ngeo2619>, 2016.

846 Reiss, D. et al.: Absolute dune ages and implications for the time of formation of gullies in Nirgal Vallis, Mars. *J. Geophys.*  
847 *Res.-Planets* 109, doi: <http://dx.doi.org/10.1029/2004JE002251>, 2004.

848 Reiss, D., Hauber, E. et al.: Terrestrial gullies and debris-flow tracks on Svalbard as planetary analogs for Mars, In: Garry,  
849 W.B. & Bleacher, J.E. (eds) *Analogues for Planetary Exploration*, *Geol. Soc. Am. Spec. Papers* 483, 165–175, doi:  
850 [https://doi.org/10.1130/2011.2483\(11\)](https://doi.org/10.1130/2011.2483(11)), 2011.

851 Rodine, J.D., Johnson, A.M.: The ability of debris, heavily freighted with coarse clastic materials, to flow on gentle slopes,  
852 *Sedimentology* 23, 213–234, doi: <https://doi.org/10.1111/j.1365-3091.1976.tb00047.x>, 1976.

853 Ryder, J.: Some aspects of the morphometry of paraglacial alluvial fans in South-central British Columbia, *Canadian Journal*  
854 *of Earth Sciences* 8: 1252-1264, doi: <https://doi.org/10.1139/e71-11>, 1971.

855 Schon, S.C., Head, J.W., Fassett, C.I.: Unique chronostratigraphic marker in depositional fan stratigraphy on Mars: Evidence  
856 for ca. 1.25 Ma gully activity and surficial meltwater origin, *Geology* 37, 207–210, doi: <http://dx.doi.org/10.1130/g25398a.1>,  
857 2009.

858 Siewert, M. B., Krautblatter, M., Christiansen, H. H., & Eckerstorfer, M.: Arctic rockwall retreat rates estimated using  
859 laboratory-calibrated ERT measurements of talus cones in Longyeardalen, Svalbard, *Earth Surface Processes and Landforms*,  
860 37(14), 1542-1555, doi: <https://doi.org/10.1002/esp.3297>, 2012.

861 Sinha, R. K., Ray, D., De Haas, T., & Conway, S. J.: Global documentation of overlapping lobate deposits in Martian gullies.  
862 *Icarus*, 352, 113979, doi: <https://doi.org/10.1016/j.icarus.2020.113979>, 2020.

863 Sinha, R. K., Vijayan, S., Shukla, A. D., Das, P., & Bhattacharya, F.: Gullies and debris-flows in Ladakh Himalaya, India: a  
864 potential Martian analogue, *Geol. Soc. Lond. Spec. Publ.* 467, 315-342, doi: <https://doi.org/10.1144/SP46>, 2019.

865 Sinha, R.K., Vijayan, S.: Geomorphic investigation of craters in Alba Mons, Mars: implications for Late Amazonian glacial  
866 activity in the region, *Planet. Space Sci.* 144:32–48, doi: <https://doi.org/10.1016/j.pss.2017.05.014>, 2017.

867 Souness, C., & Hubbard, B.: Mid-latitude glaciation on Mars, *Progress in Physical Geography*, 36(2), 238-261, doi:  
868 <https://doi.org/10.1177/030913331243>, 2012.

869 Souness, C., Hubbard, B., Milliken, R. E., & Quincey, D.: An inventory and population-scale analysis of martian glacier-like  
870 forms, *Icarus*, 217(1), 243-255, doi: <https://doi.org/10.1016/j.icarus.2011.10.020>, 2012.

871 Stock, J.D., Dietrich, W.E.: Erosion of steepland valleys by debris flow, *Geol. Soc. Am. Bull.* 118 (9/10), 1125–1148.  
872 doi:10.1130/B25902.1, 2006.

873 Stolle, A., Langer, M., Blöthe, J. H., & Korup, O.: On predicting debris flows in arid mountain belts, *Global and Planetary*  
874 *Change*, 126, 1-13, doi: <https://doi.org/10.1016/j.gloplacha.2014.12.005>, 2015.

875 Welsh, A., Davies, T.: Identification of alluvial fans susceptible to debris-flow hazards. *Landslides* 8 (2), 183–194, doi:  
876 <https://doi.org/10.1007/s10346-010-0238-4>, 2011.

877 Wilford, D. J., Sakals, M. E., Innes, J. L., Sidle, R. C., & Bergerud, W. A.: Recognition of debris flow, debris flood and flood  
878 hazard through watershed morphometrics, *Landslides*, 1(1), 61-66, doi: <https://doi.org/10.1007/s10346-003-0002-0>, 2004.

879 Yue, Z., Hu, W., Liu, B., Liu, Y., Sun, X., Zhao, Q. and Di, K.: Quantitative analysis of the morphology of martian gullies and  
880 insights into their formation, *Icarus*, 243, pp.208-221, doi: <https://doi.org/10.1016/j.icarus.2014.08.028>, 2014.

881